Shifts in permafrost ecosystem structure following a decade-long drainage increase energy transfer to the atmosphere, but reduce thaw depth

Mathias Göckede[1], Fanny Kittler[1], Min Jung Kwon[1], Ina Burjack[1], Martin Heimann[1,2], Olaf Kolle[1], Nikita Zimov[3], Sergey Zimov[3]

[1]Department Biogeochemical Systems, Max-Planck Institute for Biogeochemistry, Jena, Germany
[2]Division of Atmospheric Sciences, Department of Physics, University of Helsinki, Finland
[3]North-East Science Station, Pacific Institute for Geography, Far-Eastern Branch of Russian Academy of Science, Chersky, Republic of Sakha (Yakutia), Russia

Correspondence to: Mathias Göckede (mathias.goeckede@bgc-jena.mpg.de)

Abstract. Hydrologic conditions are a key factor in Arctic ecosystems, with strong influences on ecosystem structure and related effects on biogeophysical and biogeochemical processes. With systematic changes in water availability expected for large parts of the Northern high latitude region in the coming centuries, knowledge on shifts in ecosystem functionality triggered by altered water levels is crucial for reducing uncertainties in climate change predictions. Here, we present findings from paired ecosystem observations in Northeast Siberia that comprise a drained and a control site. At the former, the water table has been artificially lowered by up to 30 cm in summer for more than a decade. This sustained primary disturbance in hydrologic conditions has triggered a suite of secondary shifts in ecosystem properties, including vegetation community structure, snow cover dynamics, and radiation budget, all of which influence the net drainage effects. Reduced heat conductivity in dry organic soils was identified as the dominating drainage effect on energy budget and soil thermal regime. Through this effect, reduced heat transfer into deeper soil layers leads to shallower thaw depths, initially leading to a stabilization of organic permafrost soils, while the long-term effects on permafrost temperature trends still need to be assessed. At the same time, more energy is transferred back into the atmosphere in the drained area, with the largest fraction attributed to the sensible heat flux. Accordingly, this increase in vertical heat transfer will act as a positive feedback to permafrost degradation triggered by the warming of the lower atmospheric surface layer.

Keywords: Permafrost, Disturbance, Drainage, Energy Flux

1 Introduction

The current state and future evolution of Arctic permafrost, particularly its interactions with the atmosphere, are among the largest uncertainties in our understanding of the Earth's climate system (Schuur and Abbott, 2011; Stocker et al., 2013). The Arctic is one of the most susceptible regions on Earth to climate change (e.g. Serreze et al., 2000; Polyakov et al., 2003; Fyfe

5   et al., 2013; Pithan and Mauritsen, 2014), and altered climate conditions may have enormous consequences for the sustainability of its natural environment (Schuur et al., 2008; Arneth et al., 2010). Interactions between permafrost, climate, hydrology, and ecology have the potential to cause dramatic changes (e.g. McGuire et al., 2002; Hinzman et al., 2005), via mechanisms that are currently poorly monitored and therefore highly unpredictable (Heimann and Reichstein, 2008; van Huissteden and Dolman, 2012; Rawlins et al., 2015). The associated changes in the energy transfer between surface and

10 atmosphere (Eugster et al., 2000; Langer et al., 2011b, a) or the emission patterns of greenhouse gases (Koven et al., 2011) raise the need for experimental studies in this region that address the key uncertainties linked to the functioning of the Arctic in the earth-climate system (Semiletov et al., 2012).

Hydrologic conditions play a pivotal role in shaping Arctic ecosystems. Lakes and rivers in the permafrost region represent an important portion of regional net carbon exchange with the atmosphere, but net emissions over different

15 spatiotemporal scales remain highly uncertain to date (Walter-Anthony et al., 2014; Rasilo et al., 2015). Moreover, the vast carbon pool in northern permafrost regions, currently estimated at 1330-1580 petagrams of organic carbon (Schuur et al., 2015), has be accumulated over past millennia since a combination of low mean temperatures and anoxic conditions in areas with flooded or water saturated soils slowed down the decomposition of organic matter (e.g. Ping et al., 2008). Accordingly, besides warming temperatures also shifts in the water balance in this region are expected to trigger profound changes in the

20 permafrost carbon cycle (e.g. Chapin et al., 2005; Oberbauer et al., 2007). Hydrology can vary at smallest spatial scales and thus create fine-scale mosaics in surface conditions (Muster et al., 2012; 2013). Even minor differences in mean water levels can impose strong effects on e.g. vegetation and microbial community structures or soil thermal regimes (Zona et al., 2011a). It can thus be expected that flooding or draining a site will initiate profound shifts in ecosystem structure, and that the long-term impacts of the disturbance will look very different than the short term changes that can be observed immediately after

25 the event (e.g. Shaver et al., 1992).

Future shifts in hydrologic conditions in the Arctic can be triggered by altered precipitation patterns, where a general trend towards increased rainfall is predicted (Kattsov and Walsh, 2000); however, patterns will vary strongly by region (Huntington, 2006; Bintanja and Selten, 2014) so that also drier conditions can be expected within large areas. Geomorphological processes such as e.g. subsidence (Jorgenson et al., 2006; O'Donnell et al., 2012) or the formation of a

30 system of connected troughs through the preferential degradation of ice wedges in ice-rich permafrost (Serreze et al., 2000; Liljedahl et al., 2016) can lead to a lateral redistribution of water, and thus create both wetter and drier microsites within a formerly uniform ecosystem. Also, a deepening of the active layer can trigger reductions in waterlogged conditions and wetland extend in permafrost regions (Avis et al., 2011). In-depth insight into the net effect resulting from long-term changes

in hydrology therefore forms a key challenge for improved future predictions of biogeochemical cycles in Arctic ecosystems (e.g. Lupascu et al., 2014).

Over the past two decades, several studies have documented the effect of an experimental manipulation of soil hydrologic conditions on biogeochemical cycles in Arctic ecosystems (e.g. Oechel et al., 1998; Olivas et al., 2010; Natali et al., 2015). Only few of these studies examined long-term effects of manipulated water tables (e.g. Christiansen et al., 2012; Lupascu et al., 2014), and none of them explicitly addressed the net impact of hydrologic disturbance on the energy budget; only shifts in thaw depth (Zona et al., 2011a; Kim, 2015) and indirect effects of heat fluxes on the carbon cycle (Turetsky et al., 2008) were reported. To date, the only study known to the authors that examined a drainage effect on surface-atmosphere energy exchange patterns presented results on the Bowen Ratio, and found no systematic short-term shifts immediately following a drainage disturbance (Merbold et al., 2009).

Our study presents observational evidence of shifts in ecosystem properties and energy fluxes within a wet tussock tundra ecosystem in Northeast Siberia following a decade-long drainage disturbance, providing insight into the sustainability of ice-rich permafrost under future climate change. As a first major objective, we use paired observations within a drainage and a control area to quantify several secondary disturbance effects linked to lower water tables, including vegetation community, radiation budget and soil thermal regime. Our results demonstrate that drainage disturbance triggers a sequence of changes in ecosystem properties that can only fully develop over longer timeframes. In a second step, we link these shifts in ecosystem properties to year-round eddy-covariance measurements of energy exchange patterns between permafrost ecosystem and atmosphere. As a net effect, we find increased energy transfer from the surface into the lower atmosphere, mostly in form of sensible heat, which potentially poses a positive feedback effect to Arctic warming. At the same time, severe drainage of shallow organic soil layers reduces heat transfer into deeper layers, reducing thaw depths, and thus providing a mechanism to temporarily stabilize permafrost.

2 Methods

2.1 Study site and drainage experiment

Our field experiments were conducted on a wet tussock tundra site within the floodplain of the Kolyma River (68.61°N, 161.35°E), approximately 15 km south of the town of Chersky in Northeast Siberia. The area was formed by a relatively recent shift of the main channel of the Kolyma (Corradi et al., 2005), therefore the terrain is flat and no thermokarst lakes or natural drainage channels have yet formed in the vicinity of the observation sites. Still, the existing minor differences in terrain height have led to the formation of a fine-scale mosaic in microsite conditions (Figure 1), mostly triggered by redistribution of water from slightly elevated areas towards the minor depressions.

Site hydrology is strongly influenced by a flooding period in spring caused by melting of the local snow cover as well as a northward moving dam of ice floes on the main channel of the Kolyma that delays melt water runoff. Depending on the timing of snowmelt in the tributary watersheds, this process leads to standing water on the site (up to 50 cm above ground

level) in most years around late May to early June. After the flood has mostly receded, stagnant water remains in large parts of the area that only gradually decreases over the course of the growing season.

Soils consist of an organic layer of 15-20 cm overlaying alluvial mineral soils (silty clay), with some organic material also present in deeper layers following cryoturbation. More information on site climatology (Section3.1). spatiotemporal patterns in hydrology (Section 3.20) and vegetation characteristics (Section 3.3) can be found in the Results section. Further details on the study site are presented by Corradi et al. (2005), Merbold et al. (2009) and Kwon et al. (2016).

To study the effects of a lowered water table on a formerly predominantly wet permafrost ecosystem, in fall of 2004 a drainage ring of approximately 200 m diameter was installed that is connected to the nearby river (Merbold et al. (2009), see also Figure 1). Within its watershed, this drainage system caused systematic changes in the hydrologic regime, lowering the mean water table and thus shifting the natural wetlands towards conditions with dry soils close to the surface; however, in the year immediately following the disturbance, Merbold et al. (2009) did not observe any significant drainage impacts on the energy budget within this site.

2.2 Meteorological towers

We established a paired experiment over drained and undisturbed control tundra to facilitate a direct evaluation of drainage effects on ecosystem characteristics and fluxes within this permafrost ecosystem. Since July 2013, two uniformly instrumented eddy-covariance towers with instrument heights around 5 m a.g.l. (Figure 1) captured the turbulent exchange processes between surface and atmosphere continuously throughout the year. For more details regarding instrumentation setup, data processing and data quality assessment, please refer to Kittler et al. (2016).

Additional meteorological parameters used within the context of this study include air temperature (2 m a.g.l., KPK 1/6-ME-H38, Mela), precipitation (1 m a.g.l., heated tipping bucket rain gauge, Thies), and long- and shortwave radiation components (5 m a.g.l., CNR4, Kipp & Zonen). For a comprehensive survey of ancillary parameters monitored at the towers, including a detailed description in data quality assessment, please refer to Kittler et al. (2016).

For the results presented within Section 3 of this manuscript, all data were aggregated to daily timesteps.

2.3 Soil monitoring and vegetation sampling

In each of the two treatment areas (i.e. drainage and control), we set up transects of ten sampling locations placed approximately 25 m apart, yielding two transects with a total length of 225 m each (Figure 1). At each location, we measured water table depth in permanently installed perforated PVC pipes with 25 mm inner diameter. Thaw depth was assessed by pushing a metal pole into the ground. At every other site, profile probes for soil temperature with sensors at 0.05, 0.15, 0.25 and 0.35 m (Th3-s, UMS, Germany) and TDR soil moisture sensors at 0.075, 0.15 and 0.30 m below the soil surface (CS 640, 630 and 605, Campbell Scientific, USA) were permanently installed. These measurements were taken at irregular time intervals over the course of the growing season. In addition to the manual sampling, at four of the sampling locations, i.e. a

wet and a dry microsite in each of the treatment areas, soil temperatures were continuously sampled at 0.04, 0.16 and 0.64 m since August 2014.

In 2014, we applied a non-destructive point-intercept method to sample vegetation community structure, with 20 sampling spots of 0.60 x 0.60 m within each treatment. Structuring each sampling spot into a subgrid of 6x6 cells with a side length of 0.10 m, we recorded the vegetation species that intercepted a laser pointer beam when pointing downwards from each grid intersection. The final coverage fraction for each vegetation species was approximated through the relative frequency of occurrence of classes found at these intersection points. More details are provided by Kwon et al. (2016).

2.4 Site climatology

Long-term temperature trends for the Chersky region were analyzed based on data from the period 1960-2009 provided by the Berkeley Earth project (berkeleyearth.org, station ID 169921). These Berkeley Earth surface temperature (BEST) time series underwent thorough data quality filtering to e.g. flag dubious data, or exclude data biased by instrument issues. Long-term precipitation records for the period 1950-1999 were obtained from a local weather station through the NOAA online climate database (http://www.ncdc.noaa.gov/cdo-web/datasets, station ID 00025123). Since for the Chersky station virtually no precipitation records were available for the decade 2000-09, in addition to this station we analyzed long-term trends for the site Ambarchik (station ID 00025034), which is situated ~100 km to the North from Chersky and displays an almost identical mean annual course of monthly precipitation sums.

3 Results

3.1 Climate and weather

3.1.1 Seasonality in temperature and precipitation

The averaged (1960-2009) seasonal air temperature course (Figure 2, left panel) has an amplitude of ~45 °C, bounded by a minimum monthly average of -33 °C in January and a maximum of 12 °C in July. The mean annual temperature within these five decades is -11 °C. The averaged annual precipitation sum for Chersky amounts to 197 mm, with mean monthly precipitation varying between 7 mm in March and 30 mm in August (Figure 2, right panel). The bulk of the annual precipitation input is received during the summer (JJA, ~39 %) and fall (SON, ~31 %) months.

Figure 2 summarizes that the mean monthly air temperatures observed in the period 2013–15, which represent the datasets used in the subsequent sections, follow the general amplitude of the long-term seasonal course. Individual outliers tend towards the positive range, but the annual mean temperature of -10.9 °C for the period 2014/15 is only slightly above the climatological mean. Since BEST data for Chersky are currently available until November 2013, general offsets between local site-level data and long-term records can only be approximated based on a 3-month overlap period. For these three months we find a cold bias in the local data ranging between -0.53 and -1.25 °C, explaining the good agreement between

recent data years and long-term trends despite the warming trends observed in the past decade (see also Figure 3). Precipitation data display a different pattern since April 2014 (start of measurements) compared to the long-term observations. Total precipitation in 2015 amounts to just 154 mm (~71 % of the long-term budget), with a much higher fraction provided during summer (JJA: +40 %), while winter and springtime contributions are negligible in these years;

5   however, since recent wintertime precipitation measurements are persistently low at very low temperatures, these data are likely to be subject to biases caused by insufficient heating of the sensor. Accordingly, focusing just on summertime conditions our records indicate an increase in precipitation in recent years, compared to the period 1950-1999 that was used for generating the climatology.

3.1.2 Long-term climate trends

10   BEST long-term temperature trends were analyzed broken up into four seasons of three months each: springtime warming (MAM), core summer (JJA), fall freeze-up (SON), and core winter periods (DJF); the setup of these periods intentionally deviates from the definition of seasons in e.g. the climatological or plant-physiological sense, instead focuses on comparing temperature trends in different parts of the seasonal course.

      The results summarized in Figure 3 indicate heterogeneous trends over both decades and seasons. Using the 1960–69
15   temperatures as a reference, absolute values and year-to-year variability within all seasons did not change much until the end of the last century. In these first four decades of the analysis, the maximum deviation from the reference was found to be 1.01 °C (SON, 1990–1999), and only minor trends towards warmer conditions were observed for the shoulder seasons (MAM, SON) in the decades between 1970 and 2000. In contrast to this, mean temperatures in all seasons but winter display a step-change when transitioning into the 2000–2009 decade, with observed increases of 3.0 (MAM), 1.4 (JJA) and 2.8
20   (SON) °C between the 1990s and the 2000s. In spite of the abrupt nature of this transition to considerably warmer temperatures, decadal root mean square errors (RMSE) remain at the same level before and after the change. Wintertime temperatures, however, show no systematic trend over the analyzed five decades, but are subject to pronounced interannual variability in seasonal mean temperatures. The hiatus in warming trends since ~2000 corresponds to global trends for that time period (e.g. Trenberth and Fasullo, 2013), and has been linked to changes in atmospheric circulation and ocean currents
25   (Trenberth et al., 2014).

      Precipitation patterns were analyzed in the same way as described above for the temperatures (results not shown). In this case, no discernable trends were found, and decadal mean precipitation stayed within ranges of +/-15mm (JJA) and +/-7 mm (all other seasons) in comparison to the 1950–59 references. Based on Ambarchik data, also the 2000–2009 precipitation sums stayed within the same ranges as observed for the five preceding decades, again without discernable trends.

30   ### 3.2 Changes in hydrologic regime as response to drainage

Patterns in water table depth on this wet tussock tundra site are highly variable in both space and time. Accordingly, also the effect of the drainage disturbance varies with the microrelief, and changes over the course of summer. The top panels of

Figure 4 demonstrate the spatial variability of terrain height and water table depth for a time where water levels had fallen to a seasonal low (here: Jul 14, 2014). The variability of the terrain height at fine scales leads to lateral water redistribution, with the result that one out of ten observation sites at the drained transect still reflects wet conditions, while two out of ten sites in the control transect have water tables far below the surface level. Accordingly, the area affected by the drainage is not uniformly dry, but conditions have changed from predominantly wet to predominantly dry.

Temporal patterns of the drainage effect are also complex, as highlighted by the bottom panels of Figure 4. After the high water levels from the spring flooding have mostly receded towards the end of June, soil water conditions stay more or less constant across the control transect, while the drained transect displays a pronounced seasonality. For the latter, the water table drops by an average of 10 cm over the first three weeks of July 2014, resulting in dry top soil conditions for all sites but one. This drop is followed by a persistent recovery in water levels as a response to intensive rainfall (see also Figure 2) in late July and early August. Mean water levels within the drained area are always lower than those in the control area; however, as a consequence of the different sensitivity to precipitation input between drained and control transects, the net drainage effect results in water table differences between 4 cm and 15 cm (2014 observations), depending on weather conditions in the respective parts of the growing season.

3.3 Vegetation structure

In its natural state, the vegetation community of this wet tussock tundra ecosystem is dominated by common cotton grasses (*E. angustifolium*), with tussock forming sedges (*C. appendiculata* and *lugens*) closely following as the second most important species (Corradi et al., 2005; Kwon et al., 2016). This is reflected in the coverage fractions observed during our 2014 plant species assessment (Table 1), which for the control area agrees well with a 2003 plant survey that was taken before the drainage disturbance was implemented (Corradi et al., 2005, not shown). Within the drained area, the decade-long shift of the water regime has strongly reduced the abundance of cotton grasses, while tussock forming sedges as well as shrub species (mostly birches, some willows) now cover larger fractions of the surface as compared to the control.

While the plot-based vegetation inventories indicate an increase in shrubs from close to zero to about 11 percent areal coverage (Table 1), we do not yet have a final quantitative assessment on the increase in shrubs within the footprint areas of the drainage tower. As an approximation, a land-cover classification based on 2011 WorldView-2 satellite remote sensing data (see also Figure 1) indicates an increase in tall shrub coverage by about a factor of four within a 400x400 m^2 area surrounding the drainage tower (from 1.2 to 4.8%), compared to an area of the same size focusing on the control tower. Also, a doubling of areas where tussocks and shrubs are mixed (from 34 to 67%) was observed. Our datasets do not include a direct assessment of the average height of shrubs in drained and control areas; however, a comparative analysis between both towers (Figure 5) shows that drainage has led to a median increase of 16 % in summertime friction velocities. Since both sites are exposed to the same climate conditions, this shift can only be caused by increases in surface roughness conditions linked to a higher abundance of tussocks as well as more and higher shrubs.

3.4 Snow cover, albedo and radiation budget

The changes in moisture regime and vegetation structure described in Sections 0 and 0 above have a profound impact on the local radiation budget, with the most pronounced effects attributed to shifts in snow cover. While the longwave radiation budget remains virtually unchanged (data not shown), shortwave radiation is altered through changes in albedo, with distinct

5   seasonal patterns in the differences between drainage and control areas that allow to structure the 'light season' (mean daily net shortwave radiation >5 Wm^{-2}) into seven distinct sections (see Table 2 and Figure 6 for an analysis of the data year 2014).

In the snow free season, the shift in vegetation in the drainage area causes a minor but persistent increase in the albedo, which leads to a shortwave radiation budget that is lowered by about 2 Wm^{-2} throughout the summer since more energy is

10   directly reflected upwards by lighter colored surfaces. This reduction in energy input agrees with Eugster et al. (2000), who observed increases in albedo linked to the gradual decrease in soil moisture over the course of the growing season. Major changes in albedo are observed during the disappearance and buildup of a closed snow cover in spring and fall. As shown in Figure 6, in both cases the process is initiated earlier in the drainage area, an effect that was observed in all data years since the beginning of the experiment in 2013. Since the thawing period in May falls together with high incoming shortwave

15   radiation, even a few extra snow-free days lead to a strong increase in incoming energy (see also Table 2). Also the prolonged period where the snow cover starts to thin in spring leads to an energy gain for the drained terrain. Conversely, the earlier buildup of a closed snow cover in fall, as indicated by a rapidly increasing albedo, has little effect on the energy budget since incoming radiation at that time of the year is already very low.

Table 2 and Figure 6 demonstrate that a negative albedo difference between the drainage and control areas, is only

20   found during the snow melt period in spring, which makes up just about 13 % of the total time with sufficient incoming radiation for this kind of analysis (net shortwave radiation >5 Wm^{-2}). Since this short period falls together with high incoming radiation, the average impact of albedo changes on the energy budget is still positive for the drained area, with an average gain of 0.6 Wm^{-2} over the total period of almost nine months. However, excluding this short period, the radiative energy input has been reduced as a consequence of drainage and subsequent albedo changes.

25 3.5 Soil thermal regime

The changes in soil water conditions, radiation and snow cover listed above have profound consequences on the soil thermal regime within this tundra ecosystem. These effects are summarized in Figure 7, where we compare continuous observations of soil temperatures down to 0.64 m below surface level between a dry and a wet microsite within the drained transect (similar relationships between moisture and soil temperature regime were observed within the control transect). We

30   differentiate three major effects over the course of the year:

1. Drier conditions close to the surface at the dry microsite reduce the heat capacity of the organic soil. As a consequence, the upper few centimeters of the soil profile get warmer in the period June to August, with differences of up to 10 °C,

compared to the wet microsite. At the same time, low heat conductivity of dry organic soil prevents vertical heat transfer, so within the dry microsite deeper layers remain cooler for most of the period June through December.

2. Within the period December to January, the larger heat capacity linked to the higher water content in organic soil within the wet microsite extends the zero curtain period, and delays the freezing for several weeks compared to the dry microsite. Accordingly, soils under dry conditions are much colder in early winter, with temperature differences that can reach up to 10 °C.

3. In the second half of February, the soil temperature decrease within the wet microsite finally catches up with the dry site, and drops down to even colder temperatures. This effect can most likely be linked to deeper snow cover associated with taller vegetation in the dry areas of this tundra site. The resulting slightly warmer temperatures across the dry soil profile, which persist until June, were observed within both treatment areas in both years currently covered by the dataset.

To study the effects of moisture on the soil thermal regime in more detail, we analyzed time series of soil temperatures, soil moisture and thaw depth at eight selected microsites. These sites were distributed across both treatments (drained: 5 sites; control: 3 sites), covering wet and dry conditions within both areas. The dataset was collected during two experiments in summer 2015, and was subsequently aggregated into four blocks of about two weeks each (Figure 8).

Close to the surface at 5 cm depth (Figure 8, left panel), wetter conditions lead to colder soil temperatures, confirming the differences between drained and control conditions during summertime already highlighted in Figure 7, related to the lower heat capacity of dry organic soils. The temperature gradient between dry and wet microsites declines in late summer following the reduced radiative energy input (Figure 6). At 35 cm depth (Figure 8, center panel), opposite trends are observed. Here, higher soil moisture stimulates higher soil temperatures, which can be linked to the fact that dry organic soil is a poor heat conductor. So even though this soil is warmer close to the surface, compared to wet microsites, the energy is not transferred into deeper soil layers, insulating the underlying permafrost from the heat close to the surface. Gradients grow over the course of the growing season, resulting in temperature differences of almost 2 °C between dry and wet microsites at times.

Higher temperatures in deeper soil layers linked to wetter conditions clearly promote deeper thaw depths (Figure 8, right panel), with differences between dry and wet microsites increasing over the course of the growing season. In September, these differences can amount to more than 20 cm as a result of shifts in the soil water regime.

3.6 Sensible and latent heat fluxes

The changes in ecosystem properties following the drainage disturbance have profound impacts on the surface–atmosphere exchange fluxes of energy. In the following paragraphs, all numbers referring to growing season averages or differences represent results for the months June through September (see also Table 3) while results for the winter season are discussed separately further below:

1. **Net radiation:** Due to a closed snow cover that usually lasts well into the month of May, most of the radiative energy is reflected until around early June (see also Figure 6), when a steep increase in net radiation (R_{net}) is observed at both sites (Figure 9a). Systematic differences in R_{net} between drainage and control site can only be observed during those few days in spring when the snow cover disappears earlier at the drained site (Figure 9f); however, averaged over the growing season months June through September in 2014 and 2015, which largely excludes the snow melt transition, the energy input is reduced by about -1.7 Wm^{-2} (-1.8 %) caused by the higher albedo in the drainage area (see also Table 3).

2. **Sensible heat flux:** Exchange of energy between surface and atmosphere in form of sensible heat (H) displays a sawtooth pattern over the growing season correlated to the net radiation trends, with a steep incline in June followed by a gradual decrease that lasts through fall (Figure 9b). The timing between the increase in net radiation and H is not aligned, with the onset of high sensible heat fluxes in spring trailing the steep increase in R_{net} by 1-2 weeks. Differences in H between drainage and control area are scaled with the absolute values, with largest differences found in the early summer months (Figure 9g). Overall, sensible heat fluxes have systematically increased as a consequence of the drainage, with peak differences reaching up to 50 Wm^{-2} for single days in early summer, and an average growing season increase of 4 Wm^{-2} per day (+16.7 %, Table 3).

3. **Latent heat flux:** In contrast to the patterns observed for the sensible heat flux, latent heat fluxes (LE) start displaying higher values very shortly after the snow melt, but subsequently increase slowly until reaching a maximum in July (Figure 9c). For LE, we observed a pronounced interannual variability in differences between drainage and control areas (Figure 9h), which can be linked to variable weather conditions in different parts of the growing season (see discussion below). In 2014, latent heat fluxes in the drained area were lower compared to the control area by an average of -1.9 Wm^{-2} per day, which can mostly be attributed to reductions in LE in the months of June and July within the drainage. In contrast to that, during the growing season of 2015 the latent heat fluxes were higher within the drained section (average: 2.8 Wm^{-2} per day), except for a brief period immediately following the spring flooding. Averaged over both data years, this leads to a minor increase of LE within the summer months of 0.5 Wm^{-2} (+1.8 %,Table 3) within the drainage.

4. **Sum of surface-atmosphere energy exchange:** Summing up shifts in H and LE indicates a systematic trend towards higher energy fluxes from surface to atmosphere as a consequence of the drainage (Figure 9i). Mean values and temporal patterns, however, differ strongly between years. In 2014, where shifts in H and LE are of opposite sign for large parts of the summer months, the average increase in total energy fluxes is moderate (2.4 Wm^{-2} daily average). Net shifts between treatments are dominated by two short periods in early June (peak in H differences) and early August (positive offset in LE following heavy precipitation), while offsets are close to zero otherwise. In contrast to that, in 2015 the positive offsets in H and LE combine to a continuous positive difference in overall energy exchange between treatments, summing up to a daily mean of 6.6 Wm^{-2} over the four growing season months. Averaging over both years, drainage increases the summertime energy flux by 4.5 Wm^{-2} per day (+8.8 %, Table 3).

5. **Bowen-Ratio:** The Bowen-Ratio (BR), i.e. the ratio of sensible to latent heat fluxes, summarizes how radiative energy is partitioned between the two vertical energy fluxes H and LE. The higher the BR values, the more the available energy is shifted towards the sensible heat flux, which may indicate water limitations and/or drought stress. At the Chersky sites, absolute daily mean values of BR are usually highest during the early summer, then decrease until August and rise again towards the beginning of fall (Figure 9e). Smoothed offsets between drainage and control are positive throughout the summer months (Figure 9j), i.e. the share of energy transferred into sensible heat is systematically higher within the drainage area. Mean summertime Bowen Ratios, calculated based on averaged values for H and LE demonstrate that drainage increases daily mean BR by a value of 0.13 (+14.7 %, Table 3).

Wintertime fluxes do not contribute notably to net changes in the energy budget at the Chersky sites. With shortwave energy input extremely low during the polar winter and outgoing longwave radiation usually exceeding the incoming amount, R_{net} averages -11.5 Wm^{-2} for the winter months (November through March), with slightly lower values (difference of -1.6 Wm^{-2}) in the drainage area. Latent heat fluxes are virtually zero for this entire period, and sensible heat also has a slightly negative average flux of -3.4 Wm^{-2}, again with slightly lower values (difference of -1.8 Wm^{-2}) in the drainage. Accordingly, changes in R_{net} are almost perfectly balanced through the changes in energy fluxes, so that during wintertime, the aboveground energy balance (R_{net} – H – LE) is not affected by the drainage disturbance.

4 Discussion

4.1 Controls on Arctic energy balance

Previous studies have identified vegetation community, atmospheric conditions, and the underlying permafrost as major controlling factors on the biogeochemical cycles of Arctic wetland ecosystems (e.g. Rouse, 2000). Focusing on the energy budget, Eugster et al. (2000) identified the following properties as dominant features that characterize the specific feedback processes between the Arctic energy balance and climate change: short growing season with long summer days, permafrost and the existence of massive ground ice, prevalent wetlands and shallow lakes, and a nonvascular ground vegetation. All of these factors are closely linked to each other (e.g. McGuire et al., 2002), and thus the assessment of the net effect of climate change on these ecosystems needs to synthesize inter-related responses to capture the cascade of positive and negative feedback loops that affect geophysical, hydrological, and biological ecosystem characteristics (McFadden et al., 1998; Hinzman et al., 2005). This is supported by the findings from our experiment, where the impact of soil hydrology was identified as the dominant control, triggering secondary shifts in other factors and ultimately reshaping the ecosystem.

4.1.1 Vegetation impact

Many studies that examined the energy budget across ecosystem boundaries in the Arctic have identified the terrain type as the dominant control on energy flux rates as well as on the partitioning of energy between sensible, latent and soil heat fluxes (Eugster et al., 2000; Eaton et al., 2001; Beringer et al., 2005; Kasurinen et al., 2014). For example, Beringer et al.

(2005) studied a vegetation transect in Alaska, and found increasing leaf area index and decreasing albedo along the transition from arctic tundra to boreal forest ecosystems, which decreased evaporation while increasing transpiration and sensible heat fluxes. Their results demonstrate that successional changes that convert low tundra vegetation into shrub tundra or woodlands have the potential to intensify vertical energy exchange with the atmosphere, and thus create a positive
5   feedback to warmer conditions under future climate change.

The results presented in this study confirm that vegetation is a key controlling factor within the cascade of secondary shifts in ecosystem characteristics following the primary drainage disturbance. The higher abundance of shrubs, promoted by drier and warmer conditions in shallow soil layers within the drainage area, exerts the most obvious effect on the snow cover regime: first, shrubs and tussocks capture the horizontally drifting snow more effectively than cotton grass meadows in the
10 control tundra sections, leading to an earlier and deeper accumulation of a closed snow cover in fall (e.g. Sturm et al., 2001a; 2005b), and subsequently to warmer soil conditions in the winter season; second, shrubs sticking out of the otherwise closed snow cover absorb and re-emit the high incoming radiation in April/May, and thus contribute to the earlier snow melt observed within the drainage area (Sturm et al., 2005a; 2005b; Pomeroy et al., 2006). During summer, it is likely that ground shading by shrub canopies counteracts the observed warming in shallow soil layers during summer (e.g. McFadden et al.,
15 1998); however, based on our dataset, this effect could not be separated from the soil moisture impact on soil temperatures.

Both plot surveys and gridded maps do not include information on vegetation height. Still, the available ground-based and remote sensing information on shifts in vegetation community structure provides strong evidence that drainage induces shifts towards taller vegetation that play a major role in the overall transformation of the ecosystem structure following the drainage disturbance. During summertime, our eddy-covariance fluxes indicate an omnidirectional increase in mechanically
20 generated turbulence (e.g. Stull, 1988) at the drainage tower (as represented by the friction velocity, Figure 5), compared to the control tower, indicating that higher vegetation surrounding that tower intensifies turbulent exchange processes between surface and atmosphere.

The virtual absence of mosses at our observation sites (~1.8% in both transects, data not shown) is also expected to influence energy flux rates and soil thermal regime. Moss cover usually dominates the surface in high latitudes, and has been
25 shown to play a key role in modifying temperature and moisture conditions in Arctic soils (Beringer et al., 2001; Zona et al., 2011b; Kim et al., 2014). Evaporation from mosses contributes a significant portion of the latent heat flux in Arctic ecosystems (McFadden et al., 2003; Beringer et al., 2005). Moss insulation reduces the soil heat flux and increases energy exchange with the atmosphere (Beringer et al., 2001), similar to the insulation effect of dry organic soil that was observed in the present study. It can therefore be assumed that drainage could further reinforce the moss-cover effect on energy flux
30 partitioning and soil thermal regime, as long as the drained soil can still sustain the moss layer.

4.1.2 Atmospheric impact

Numerous studies identified atmospheric forcing as the most important control on the energy budget of individual high latitude ecosystems in the absence of vegetation shifts (e.g. Rouse et al., 1992; Harazono et al., 1998; Kodama et al., 2007;

Boike et al., 2008; Langer et al., 2011b). Precipitation anomalies were found to be a major determinant for interannual variability in energy partitioning (Boike et al., 2008), and Rouse et al. (1992) listed variations in the total amount of summertime precipitation as a control for active layer depth development. Synoptic patterns exerted a strong influence on energy fluxes in both Alaskan (Harazono et al., 1998) and Siberian (Kodama et al., 2007; Boike et al., 2008; Langer et al.,

5   2011b) study domains: Onshore winds coming from the ocean, characterized by cold and wet conditions, promote sensible heat fluxes since they increase the temperature gradient between surface and atmosphere. Warm and dry offshore winds, however, usually decrease the sensible heat flux. Also the impact of cloud cover on the longwave radiation budget had an important influence on soil temperatures and freeze-back patterns in fall (Langer et al., 2011b).

    Short-term shifts in weather conditions, such as e.g. a warm bias in August 2014 (see Figure 2), exerted only a

10   dampened influence on the seasonal trajectories of the sensible heat flux. In contrast, an average long-term reduction in net radiation of about 5 % during the period June through September 2015, compared to 2014, decreased the H budget by about 5 %. No systematic differences in the interannual variability of H were observed between drained and control areas, i.e. overall percentage flux rate reductions were of equal magnitude, and both areas reacted uniformly to changes in atmospheric forcings.

15   Regarding the latent heat flux, in accordance with the results presented by Boike et al. (2008) our results indicate an influence of precipitation patterns on interannual variability in LE, particularly in late summer and within the drainage section of our study area. For example, two isolated heavy rainfall events in late July and early August 2014 led to partially waterlogged conditions within the drainage ring (Figure 4). Together with the higher energy availability for H and LE as a result of reduced heat transfer into deeper layers after drainage, these conditions yielded a strong increase in

20   evapotranspiration rates. Moreover, in contrast to the sensible heat flux we found evapotranspiration rates highly susceptible to day-to-day variability in net radiative energy input. Regarding interannual variability, we derived opposing trends in LE within drained and control areas: compared to the 2014 growing season budget, in 2015 latent heat flux rates increased by an average of ~5 % in the drained areas, while the control fluxes decreased by about 12 %.

    Comparing weather conditions and energy fluxes between 2014 and 2015, the reduction in net radiation input in 2015

25   led to a pronounced reduction in vertical energy transfer to the atmosphere in the control section (about 8 %, combining H and LE), while the net change in turbulent fluxes in the drained area was close to zero (-0.6 %). These findings suggest that the timing of shifts in weather conditions played an important role for latent heat fluxes within the drainage section, and dominates interannual variability: The slightly warmer conditions in June and July of 2015, in combination with the frequent occurrence of light to moderate rainfall events, resulted in higher latent heat fluxes in this period in the drained section,

30   compared to 2014. In contrast, the major reduction in net radiation in August, together with cooler and drier conditions, did not have such a strong effect since soils in the drained area had already largely dried out by then.

    Synoptic influences were not analyzed in detail in the context of this study. Our focus was placed on the differences in ecosystem structure and surface-atmosphere energy exchange between a drained and a control observation site. Since both sites were placed only approximately 600 m apart, it can be assumed that both are exposed to the same atmospheric forcing.

A direct comparison of weather conditions measured at both towers, including air temperatures, humidity, pressure and precipitation, resulted in no systematic offsets going beyond the calibration accuracy of the employed instrumentation.

4.1.3 Impact of permafrost

A primary characteristic of permafrost landscapes is that the ice-rich frozen layer inhibits vertical water losses, preserving water-logged conditions during large parts of the summer, and thus facilitating the establishment of wetlands even in areas with relatively low precipitation input (Rouse, 2000). Within permafrost landscapes, a large portion of the net energy input from radiation is used to thaw the frozen ground, and increase the thaw depth over the course of the growing season (e.g. Lund et al., 2014). Permafrost constitutes a substantial heat sink, reducing the soil temperatures and also the energy available to feed turbulent heat flux exchange with the atmosphere (Eugster et al., 2000; Langer et al., 2011b). Accordingly, permafrost acts as an efficient buffer against the intensification of energy exchange that might be triggered by a warmer future climate in high latitude regions, but this controlling mechanism would be reduced in case the thaw depth increases (Lund et al., 2014). Another particular feature of northern permafrost soils is that the very cold frozen ground generates a downward directed heat flux from the snow in spring. This increases the amount of energy required to melt the snowpack, and accordingly delays melt (Eugster et al., 2000). We speculate that the warmer soil conditions found within the drainage area in late winter are the result of better ground insulation through increased snow depth captured by higher shrubs. This effect reduces the downward heat flux, and therefore also contributes to an earlier snowmelt.

For the reasons listed above, wet permafrost ecosystems are often characterized by a large fraction of the soil heat flux in the energy budget (Boike et al., 2003; Langer et al., 2011b) that can be of the same order of magnitude as latent and sensible heat fluxes (Eugster et al., 2000). The partitioning of net radiation in permafrost landscapes is particularly sensitive towards the moderation of bulk surface resistance by the vegetation, and the thermal conductivity of shallow soil layers (Harding et al., 2002; Liljedahl et al., 2011). In the presented study, soil heat fluxes were not measured directly, so their magnitude can only be approximated based on the difference of energy supply from net radiation and energy demand for latent and sensible heat fluxes. This residual amounted to 40–48 % depending on data year and site, or 20–28 % assuming that 20% of the net radiation is attributed to an unclosed energy balance (Foken et al., 2011) or additional energy sinks such as e.g. heat storage in water (Harazono et al., 1998). While residuals in 2014 and 2015 were similar in the control area, values differed by about 10 % in the drained section, highlighting that the permafrost buffer against variability in atmospheric forcing has been weakened as a consequence of the long-term drainage.

4.1.4 Impact of soil hydrology

The moisture and thermal regulation of Arctic wetland ecosystems is strongly influenced by the presence of an organic soil layer, which features an extremely large water content when wet, and equally large air content when dry (Rouse, 2000). Water saturation conditions affect heat flux rates into soils, and thus also alter the net heat exchange between ecosystem and atmosphere, as well as thaw depth (Jorgenson et al., 2010; Subin et al., 2013). Moreover, waterlogged conditions can

increase solar absorption, contributing to increased thaw depths and potentially to a subsequent lowering of the water table with respect to the surface (Olivas et al., 2010). Conversely, lowering the water table can also preserve moisture in the ecosystem in the absence of plants with high leaf area index and deep roots, since higher albedo reduces net radiation, and poor heat conductivity in dry soils keeps deeper layers colder (Eugster et al., 2000).

5   We found both direct and indirect effects of shifts in soil hydrology on the energy budget of our study site, with the latter likely to have a stronger impact on the long-term trajectory of this permafrost ecosystem than the former. The combined impact of the most prominent indirect effects, i.e. the shifts in vegetation community structure and snow cover regime, will be discussed in more detail in the following section. Direct effects comprise the decrease in both heat capacity as well as heat conductivity when drying out organic soils, which in our case resulted in a reduction of heat transfer into the
10   soil, and an increase of turbulent energy exchange with the atmosphere. The observed patterns between soil water content and progress of thaw depth over the course of the growing season agree well with findings previously reported for Arctic ecosystems in Alaska (Hinzman et al., 1991; Shiklomanov et al., 2010; Sturtevant et al., 2012). A second direct effect of drier conditions in shallow soil layers is a shift in energy partitioning towards higher Bowen Ratios, i.e. a larger portion attributed to sensible heat fluxes. Also, after drainage particularly the latent heat fluxes become more dependent on short-
15   term atmospheric forcing, with strong variability observed in LE rates related to precipitation input.

Regarding the net effect of dry soils on soil heat fluxes and thermal regimes, different pathways are possible, depending largely on soil type and the severity of the disturbance. Rouse et al. (1992) observed that higher temperatures and associated moderate increases in evapotranspiration moved water tables beneath the surface, but the peat soils at their study site remained wet. As a result, heat conductivity decreased less rapidly than heat capacity while the thermal diffusivity was
20   enhanced, which led to deeper thaw depth with warm and dry climate conditions. In contrast, Bonan et al. (1990) postulated that the greater evapotranspiration accompanying climate warming would dry out the surface organic layer, causing a reduction of soil heat fluxes and thus stabilize the existence of permafrost. Our observation of cooler summertime temperatures in deeper soil layers following drainage, and a substantial reduction of thaw depth in the drained section, support the statement by Bonan et al. (1990); however, including secondary drainage effects, where e.g. the combination of
25   higher vegetation and higher snow pack leads to a warmer soils during winter, over longer timeframes drainage may also lead to a gradual warming of soil temperatures, and therefore contribute to permafrost degradation.

4.2 Implications for feedback processes with climate change

4.2.1 Interrelated ecosystem responses

Sophisticated numerical models are needed for assessing the complex feedback processes between permafrost ecosystems
30   and climate change, but is unclear yet which level of detail these models need to represent (Eugster et al., 2000). Our findings indicate that process-based models representing permafrost ecosystems to a high degree of detail would be required for this objective. We found direct effects of the primary drainage disturbance on the energy budget of our study site, but

also secondary effects based on shifts in other ecosystem properties following the lowered water tables. Also interactions between secondary effects were observed, including feedback processes to the primary drainage. Neglecting this network of positive and negative feedback loops on permafrost ecosystem energy budgets will likely lead to biased net effects, and therefore distort both the simulations regarding the sustainability of individual high latitude ecosystems under climate
5   change, as well as their relevance at regional to global scales.

The specific hydrologic conditions created by permafrost ecosystems, characterized by a barrier to infiltration posed by the frozen ground, provided the prerequisite to form the original wet tussock tundra ecosystem. Regarding the primary disturbance, i.e. the lowering of the soil water table, impacts on the ecosystem were initially restricted to shifts in the partitioning of energy between sensible, latent and soil heat fluxes during summertime. As a direct secondary effect, a taller
10   vegetation community with higher aerodynamic roughness was established, causing higher turbulent exchange fluxes and also a slightly higher albedo in summer. The vegetation shift then triggered substantial changes in the snow cover regime, with higher albedo and warmer soils in late winter and spring, and an energy pulse in early summer related to the expedited snow melt. Every single effect will influence the net annual energy budget of this permafrost ecosystem, and accordingly they can only be analyzed as a network of closely linked properties when assessing the net impact of drainage disturbance.

15   One particularly interesting network effect of combined shifts in ecosystem properties is the interaction between drainage and vegetation shifts. The increased abundance of shrubs in high latitude regions has been studied extensively (e.g. Sturm et al., 2001b; Myers-Smith et al., 2011; DeMarco et al., 2014a), and multiple links with e.g. snow cover (Sturm et al., 2001a; Pomeroy et al., 2006), radiation regime (Bewley et al., 2007) and nutrient cycling (Myers-Smith and Hik, 2013; DeMarco et al., 2014b) have been identified. Regarding soil temperatures, the isolated assessment of shrub expansion
20   indicates that capturing of drifting snow by shrubs increases soil temperatures in winter, while shading decreases them in summer (e.g. Sturm et al., 2001a). Assessing the net impact of these opposing effects depends on details like e.g. shrub density, complicating the evaluation of this effect at landscape to pan-Arctic level. Including a drainage effect, as studied in our experiment, adds even more complexity: During winter, the shifts in snow cover caused by the taller vegetation still persist, but the warming effect is modulated by the low heat capacity of dry organic soil, which leads to colder soil
25   temperatures in early winter. During summer, in shallow layers the warming triggered by the low heat capacity of dry organic soil dominates over the shading effect of the shrub canopy, while in deeper layers the shrub cooling effect is reinforced by low heat conductivity. Accordingly, compared to the isolated assessment of shrub expansion, a drained permafrost ecosystem with a higher abundance of shrubs experiences less warming in winter, and also shows colder temperatures in deeper layers in summer.

30   The severity of the drainage needs to be considered when interpreting the outcome of hydrologic disturbance effects. As summarized in the introduction, many studies have treated the impact of a lowered water table on biogeochemical cycles in permafrost ecosystems; however, for most of them the water table was lowered less than 10 cm, so the differences before and after disturbance were not as pronounced as to be expected after the formation of a trough system following the degradation of ice-rich permafrost. According to Rouse et al. (1992), moist organic soils can still act as good heat

conductors, so an intensification of energy exchange with the atmosphere and a corresponding reduction of thaw depth, as observed in our experiment, can only be found after a dramatic shift in soil water tables that largely dry out the shallow organic layers. Accordingly, gradually drying out tundra soils does not lead to a corresponding smooth transition from one state of energy flux partitioning to another, but instead it can be assumed that a tipping point in soil moisture levels exist

5 that, once reached, switches from one state to another in a non-linear mode.

4.2.2 Consideration of long-term effects

As pointed out in the previous section, a superposition of primary and secondary disturbance effects, and their interactions, generates the net impact of the drainage disturbance on the energy budget. In this context, temporal aspects need to be considered as well when interpreting the results. Even though the primary disturbance, the installation of the drainage ditch

10 system on our study site, acted immediately on the soil water table, other key components, most importantly the vegetation community structure, could only gradually adjust to the new environmental conditions over the course of years. As long as follow-up effects such as the changes in snow cover regime have not yet been established, the net effect would therefore have been found to be very different in the years immediately following the disturbance, compared to our results from about 10 years later. At the same time, it can be assumed that the system is even now not fully equilibrated towards the new

15 conditions, and further shifts in e.g. shrub coverage fraction and canopy height can be expected for the long-term trajectory of this site. Still, we expect that the major elements of change are already established by now, and no major shifts in the overall functionality of the energy budget feedback processes are expected for the future.

Another factor with a long-term trajectory regarding the response towards drainage disturbance is temperature trends in deeper soil layers. Throughout the studied section of the soil profile, we observed alternating periods dominated by warming

20 or cooling over the course of the year. While the strong warming during summer appears to dominate the annual thermal regime within shallow soil layers, in deeper soil layers the impact on long-term temperature trajectories is more complicated to assess: cooling down of soils in winter has been reduced here, probably linked to the improved snow insulation, while in summer the insulation by dry organic soils prevents vertical heat transfer, thus keeping deeper layers cooler. Whether or not the wintertime warming will be substantial enough to dominate over the summertime cooling, and therefore also have an

25 effect on the propagation of thaw depth, cannot be evaluated with the currently available database. An assessment of the long-term temperature trends would either require a suitable process-based modeling framework, or longer-term temperature observations, ideally including deeper boreholes, and thus is beyond the objectives of this study.

4.2.3 Implications for Arctic climate change

An increase in sensible heat flux rates as a response to shifts in the partitioning of the available net radiation is the most

30 direct pathway to change the temperature of the atmospheric boundary layer (Eugster et al., 2000; Lund et al., 2014). This statement is supported by Chapin et al. (2000), who expect a high potential for positive feedbacks between land-atmosphere energy exchange and regional temperature changes throughout high-latitude regions, disregarding potential shifts in land

cover structure. Eugster et al. (2000) therefore count the unknown magnitudes of changes in energy partitioning as well as the lack of long-term energy balance data from Siberia among the most important uncertainties for assessment of susceptibility and vulnerability of Arctic ecosystems to climate change.

5   Our experiment triggered an artificial lateral redistribution of water, converting a formerly uniform wet tussock tundra ecosystem into severely drained terrestrial areas intersected by a drainage channel. This approach mimics the preferential degradation of ice wedges in ice-rich permafrost under climate change, which can lead to the formation of a system of connected troughs (Serreze et al., 2000; Liljedahl et al., 2016). Our results can therefore provide observational evidence of energy budget shifts that can be expected in regions susceptible for this type of degradation. Ice-rich permafrost (Yedoma) covers large parts of the North American and Siberian Arctic (e.g. Strauss et al., 2013), and in the Siberian plains has been

10   found to contain very high ice contents that made up 40 to 70% of the soil volume (Zimov et al., 1997). It can be expected that geomorphological evolution and hydrological responses to permafrost degradation as a result of longer-term effects of a warming Arctic climate (e.g. Hinzman et al., 2005) will constitute a large-scale phenomenon with potential pan-Arctic and even global feedback implications on climate change.

      Regional changes in energy fluxes will probably interact with the carbon cycle by changing disturbance regime,

15   regional temperature and precipitation, and the depth of the boundary layer (Chapin et al., 2000). Moreover, shifts in energy budgets may also alter the delicate patterns of regional scale energy transfer within the Arctic and beyond. The redistribution of energy from certain regions in the Arctic and boreal zone to northern areas which is observed under current conditions, e.g. heat flows from Alaska in both northerly and easterly directions, may be increased under a warming climate whenever the energy transfer from surface to atmosphere increases (Eugster et al., 2000). Accordingly, the effects of shifts in energy

20   exchange patterns following the degradation of ice-rich permafrost will not be restricted to these areas, but are likely to exert effects of substantial magnitude at the pan-Arctic scale.

4.3 Data quality considerations

All datasets presented within the context of this study were based on the same instrumentation, as well as a uniform data processing and quality assessment routine, for both drainage and control sites. Manual measurements such as vegetation

25   community studies, or measurement of active layer depth and water table depth, were carried out by the same persons in both study areas within each specific observation period, so that also here site intercomparison results cannot be subject to systematic errors based on subjective decisions by the observer. All datasets, including eddy-covariance fluxes, slow meteorology and manual sampling, have undergone a thorough quality assessment protocol (Kittler et al., 2016; Kwon et al., 2016), which included plausibility checks based on the intercomparison of observations between both study areas. Still, it

30   cannot be ruled out that parts of the absolute values presented here are subject to systematic offsets; however, since both drainage and control datasets should be affected by such systematic offsets in the same way, the differences between these datasets will not be affected, and can thus be fully attributed to drainage effects on ecosystem characteristics and energy flux rates.

5 Conclusion

Degradation of ice-rich permafrost under future climate change holds the potential to transform geomorphological and hydrological characteristics within large parts of the Arctic. Persistently drier or wetter conditions may alter ecosystem structure dramatically, and lead to systematic shifts in biogeophysical and biogeochemical processes. Both the effects of

5 long-term equilibration and non-linear feedback processes between shifts in ecosystem components complicate the assessment of the net impact of this type of disturbance, therefore the long-term trajectory of ice-rich permafrost ecosystems in the Arctic is highly uncertain to date.

We presented observational evidence on the potential long-term consequences of sustained drainage in a previously wet tussock tundra ecosystem in Northeast Siberia. Our multi-disciplinary datasets indicate that a decade-long lowering of the

10 water table triggers a cascade of secondary changes, including shifts towards taller vegetation, modification of the snow-cover period, and profound shifts in soil temperatures. Warmer conditions were found throughout the soil profile towards the end of winter; during summer, however, the low heat capacity of dry organic soils led to warmer conditions in shallow layers, while at the same time poor heat conductivity kept deeper layers colder. With dry organic soils acting as an efficient insulator, through this mechanism drainage reduces thaw depth, and thus can initially protect deep permafrost carbon pools

15 from degradation under warmer climate conditions; however, the net impact of wintertime warming and summertime cooling on long-term permafrost temperature trends following drainage still remains to be assessed.

With heat transfer into the soil systematically reduced, the primary drainage disturbance in combination with related secondary changes led to a sustained increase in energy transfer back to the atmosphere (see also Figure 10). Even though higher albedo following vegetation shifts slightly lowered the net radiation input, mean sensible heat flux rates strongly

20 increased in the drainage area, while averaged latent heat fluxes remained largely stable. We observed an average shift of +4.5 Wm^{-2} (+8.8 %) in the sum of turbulent vertical heat transfer to the atmosphere, averaged over the summer months of 2014/15. With the bulk of this increase attributed to the sensible heat flux, drainage raised the Bowen Ratio by ~15 %. This intensification of heat transfer to the atmosphere following drainage constitutes a positive feedback with climate warming, and can thus aggravate climate change impacts once the degradation of ice-rich permafrost has initiated hydrologic

25 redistribution.

Acknowledgements

This work was supported through funding by the European Commission (PAGE21 project, FP7-ENV-2011, Grant Agreement No. 282700, and PerCCOM project, FP7-PEOPLE-2012-CIG, Grant Agreement No. PCIG12-GA-201-333796), the German Ministry of Education and Research (CarboPerm-Project, BMBF Grant No. 03G0836G), and the AXA Research

30 Fund (PDOC_2012_W2 campaign, ARF fellowship M. Göckede). The authors appreciate the contribution of staff members of the Northeast Scientific Station in Chersky for facilitating the field experiments, especially Galina Zimova and Nastya Zimova. We would also like to thank the administration and service departments within the Max-Planck-Institute for

Biogeochemistry, most notably the Field Experiments & Instrumentation group, for their contributions to planning and logistics, and for supporting field work activities.

We applied sequence-determines-credit (authors 1-3) and equal-contribution (alphabetical sequence, all other authors) methods for the order of authors.

5 **References**

Arneth, A., Sitch, S., Bondeau, A., Butterbach-Bahl, K., Foster, P., Gedney, N., de Noblet-Ducoudre, N., Prentice, I. C., Sanderson, M., Thonicke, K., Wania, R., and Zaehle, S.: From biota to chemistry and climate: towards a comprehensive description of trace gas exchange between the biosphere and atmosphere, Biogeosciences, 7, 121-149, 2010.

Avis, C. A., Weaver, A. J., and Meissner, K. J.: Reduction in areal extent of high-latitude wetlands in response to permafrost
10 thaw, Nat. Geosci., 4, 444-448, 2011.

Beringer, J., Lynch, A. H., Chapin, F. S., Mack, M., and Bonan, G. B.: The representation of arctic soils in the land surface model: The importance of mosses, J. Clim., 14, 3324-3335, 2001.

Beringer, J., Chapin, F. S., Thompson, C. C., and McGuire, A. D.: Surface energy exchanges along a tundra-forest transition and feedbacks to climate, Agr. Forest Meteorol., 131, 143-161, 2005.

15 Bewley, D., Pomeroy, J. W., and Essery, R. L. H.: Solar radiation transfer through a subarctic shrub canopy, Arct. Antarct. Alp. Res., 39, 365-374, 2007.

Bintanja, R., and Selten, F. M.: Future increases in Arctic precipitation linked to local evaporation and sea-ice retreat, Nature, 509, 479-482, 2014.

Boike, J., Roth, K., and Ippisch, O.: Seasonal snow cover on frozen ground: Energy balance calculations of a permafrost site
20 near Ny-Alesund, Spitsbergen, J. Geophys. Res.-Atmos., 108, 2003.

Boike, J., Wille, C., and Abnizova, A.: Climatology and summer energy and water balance of polygonal tundra in the Lena River Delta, Siberia, J. Geophys. Res.-Biogeo., 113, 2008.

Bonan, G. B., Shugart, H. H., and Urban, D. L.: The sensitivity of some high-latitude boreal forests to climatic parameters, Clim. Change, 16, 9-29, 1990.

25 Chapin, F. S., McGuire, A. D., Randerson, J., Pielke, R., Baldocchi, D., Hobbie, S. E., Roulet, N., Eugster, W., Kasischke, E., Rastetter, E. B., Zimov, S. A., and Running, S. W.: Arctic and boreal ecosystems of western North America as components of the climate system, Glob. Change Biol., 6, 211-223, 2000.

Chapin, F. S., Sturm, M., Serreze, M. C., McFadden, J. P., Key, J. R., Lloyd, A. H., McGuire, A. D., Rupp, T. S., Lynch, A. H., Schimel, J. P., Beringer, J., Chapman, W. L., Epstein, H. E., Euskirchen, E. S., Hinzman, L. D., Jia, G., Ping, C. L.,
30 Tape, K. D., Thompson, C. D. C., Walker, D. A., and Welker, J. M.: Role of land-surface changes in Arctic summer warming, Science, 310, 657-660, 2005.

Christiansen, C. T., Svendsen, S. H., Schmidt, N. M., and Michelsen, A.: High arctic heath soil respiration and biogeochemical dynamics during summer and autumn freeze-in - effects of long-term enhanced water and nutrient supply, Glob. Change Biol., 18, 3224-3236, 2012.

35 Corradi, C., Kolle, O., Walter, K., Zimov, S. A., and Schulze, E. D.: Carbon dioxide and methane exchange of a north-east Siberian tussock tundra, Glob. Change Biol., 11, 1910-1925, 2005.

DeMarco, J., Mack, M. C., and Bret-Harte, M. S.: Effects of arctic shrub expansion on biophysical vs. biogeochemical drivers of litter decomposition, Ecology, 95, 1861-1875, 2014a.

DeMarco, J., Mack, M. C., Bret-Harte, M. S., Burton, M., and Shaver, G. R.: Long-term experimental warming and nutrient additions increase productivity in tall deciduous shrub tundra, Ecosphere, 5, 2014b.

Eaton, A. K., Rouse, W. R., Lafleur, P. M., Marsh, P., and Blanken, P. D.: Surface energy balance of the western and central Canadian subarctic: Variations in the energy balance among five major terrain types, J. Clim., 14, 3692-3703, 2001.

5 Eugster, W., Rouse, W. R., Pielke, R. A., McFadden, J. P., Baldocchi, D. D., Kittel, T. G. F., Chapin, F. S., Liston, G. E., Vidale, P. L., Vaganov, E., and Chambers, S.: Land-atmosphere energy exchange in Arctic tundra and boreal forest: available data and feedbacks to climate, Glob. Change Biol., 6, 84-115, 2000.

Foken, T., Aubinet, M., Finnigan, J. J., Leclerc, M. Y., Mauder, M., and U, K. T. P.: Results of a panel discussion about the energy balance closure correction for trace gases, B. Am. Meteorol. Soc., 92, ES13-ES18, 2011.

10 Fyfe, J. C., von Salzen, K., Gillett, N. P., Arora, V. K., Flato, G. M., and McConnell, J. R.: One hundred years of Arctic surface temperature variation due to anthropogenic influence, Sci. Rep., 3, 2013.

Harazono, Y., Yoshimoto, M., Mano, M., Vourlitis, G. L., and Oechel, W. C.: Characteristics of energy and water budgets over wet sedge and tussock tundra ecosystems at North Slope in Alaska, Hydrol. Proc., 12, 2163-2183, 1998.

Harding, R. J., Jackson, N. A., Blyth, E. M., and Culf, A.: Evaporation and energy balance of a sub-Arctic hillslope in 15 northern Finland, Hydrol. Proc., 16, 1419-1436, 2002.

Heimann, M., and Reichstein, M.: Terrestrial ecosystem carbon dynamics and climate feedbacks, Nature, 451, 289-292, 2008.

Hinzman, L. D., Kane, D. L., Gieck, R. E., and Everett, K. R.: Hydrologic and thermal properties of the active layer in the Alaskan Arctic, Cold Reg. Sci. Technol., 19, 95-110, 1991.

20 Hinzman, L. D., Bettez, N. D., Bolton, W. R., Chapin, F. S., Dyurgerov, M. B., Fastie, C. L., Griffith, B., Hollister, R. D., Hope, A., Huntington, H. P., Jensen, A. M., Jia, G. J., Jorgenson, T., Kane, D. L., Klein, D. R., Kofinas, G., Lynch, A. H., Lloyd, A. H., McGuire, A. D., Nelson, F. E., Oechel, W. C., Osterkamp, T. E., Racine, C. H., Romanovsky, V. E., Stone, R. S., Stow, D. A., Sturm, M., Tweedie, C. E., Vourlitis, G. L., Walker, M. D., Walker, D. A., Webber, P. J., Welker, J. M., Winker, K., and Yoshikawa, K.: Evidence and implications of recent climate change in northern Alaska and other arctic 25 regions, Clim. Change, 72, 251-298, 2005.

Huntington, T. G.: Evidence for intensification of the global water cycle: Review and synthesis, J. Hydrol., 319, 83-95, 2006.

Jorgenson, M. T., Shur, Y. L., and Pullman, E. R.: Abrupt increase in permafrost degradation in Arctic Alaska, Geophys. Res. Lett., 33, 2006.

30 Jorgenson, M. T., Romanovsky, V., Harden, J., Shur, Y., O'Donnell, J., Schuur, E. A. G., Kanevskiy, M., and Marchenko, S.: Resilience and vulnerability of permafrost to climate change, Can. J. Forest Res., 40, 1219-1236, 2010.

Kasurinen, V., Alfredsen, K., Kolari, P., Mammarella, I., Alekseychik, P., Rinne, J., Vesala, T., Bernier, P., Boike, J., Langer, M., Belelli Marchesini, L., van Huissteden, K., Dolman, H., Sachs, T., Ohta, T., Varlagin, A., Rocha, A., Arain, A., Oechel, W., Lund, M., Grelle, A., Lindroth, A., Black, A., Aurela, M., Laurila, T., Lohila, A., and Berninger, F.: Latent heat 35 exchange in the boreal and arctic biomes, Glob. Change Biol., n/a-n/a, 2014.

Kattsov, V. M., and Walsh, J. E.: Twentieth-century trends of arctic precipitation from observational data and a climate model simulation, J. Clim., 13, 1362-1370, 2000.

Kim, Y., Nishina, K., Chae, N., Park, S. J., Yoon, Y. J., and Lee, B. Y.: Constraint of soil moisture on CO_2 efflux from tundra lichen, moss, and tussock in Council, Alaska, using a hierarchical Bayesian model, Biogeosciences, 11, 5567-5579, 40 2014.

Kim, Y.: Effect of thaw depth on fluxes of CO_2 and CH_4 in manipulated Arctic coastal tundra of Barrow, Alaska, Sci. Total Environ., 505, 385-389, 2015.

Kittler, F., Burjack, I., Corradi, C. A. R., Heimann, M., Kolle, O., Merbold, L., Zimov, N., Zimov, S. A., and Göckede, M.: Impacts of a decadal drainage disturbance on surface-atmosphere fluxes of carbon dioxide in a permafrost ecosystem, Biogeosciences Discuss., 2016, 1-38, 2016.

Kodama, Y., Sato, N., Yabuki, H., Ishii, Y., Nomura, M., and Ohata, T.: Wind direction dependency of water and energy
5 fluxes and synoptic conditions over a tundra near Tiksi, Siberia, Hydrol. Proc., 21, 2028-2037, 2007.

Koven, C. D., Ringeval, B., Friedlingstein, P., Ciais, P., Cadule, P., Khvorostyanov, D., Krinner, G., and Tarnocai, C.: Permafrost carbon-climate feedbacks accelerate global warming, Proc. Natl. Acad. Sci. USA, 108, 14769-14774, 2011.

Kwon, M. J., Heimann, M., Kolle, O., Luus, K. A., Schuur, E. A. G., Zimov, N., Zimov, S. A., and Göckede, M.: Long-term drainage reduces CO_2 uptake and increases CO_2 emission on a Siberian floodplain due to shifts in vegetation community
10 and soil thermal characteristics, Biogeosciences, 13, 4219-4235, 2016.

Langer, M., Westermann, S., Muster, S., Piel, K., and Boike, J.: The surface energy balance of a polygonal tundra site in northern Siberia - Part 2: Winter, Cryosphere, 5, 509-524, 2011a.

Langer, M., Westermann, S., Muster, S., Piel, K., and Boike, J.: The surface energy balance of a polygonal tundra site in northern Siberia - Part 1: Spring to fall, Cryosphere, 5, 151-171, 2011b.

15 Liljedahl, A. K., Hinzman, L. D., Harazono, Y., Zona, D., Tweedie, C. E., Hollister, R. D., Engstrom, R., and Oechel, W. C.: Nonlinear controls on evapotranspiration in arctic coastal wetlands, Biogeosciences, 8, 3375-3389, 2011.

Liljedahl, A. K., Boike, J., Daanen, R. P., Fedorov, A. N., Frost, G. V., Grosse, G., Hinzman, L. D., Iijma, Y., Jorgenson, J. C., Matveyeva, N., Necsoiu, M., Raynolds, M. K., Romanovsky, V. E., Schulla, J., Tape, K. D., Walker, D. A., Wilson, C. J., Yabuki, H., and Zona, D.: Pan-Arctic ice-wedge degradation in warming permafrost and its influence on tundra
20 hydrology, Nat. Geosci., 9, 312-+, 2016.

Lund, M., Hansen, B. U., Pedersen, S. H., Stiegler, C., and Tamstorf, M. P.: Characteristics of summer-time energy exchange in a high Arctic tundra heath 2000-2010, Tellus B, 66, 2014.

Lupascu, M., Welker, J. M., Seibt, U., Maseyk, K., Xu, X., and Czimczik, C. I.: High Arctic wetting reduces permafrost carbon feedbacks to climate warming, Nat. Clim. Change, 4, 51-55, 2014.

25 McFadden, J. P., Chapin, F. S., and Hollinger, D. Y.: Subgrid-scale variability in the surface energy balance of arctic tundra, J. Geophys. Res.-Atmos., 103, 28947-28961, 1998.

McFadden, J. P., Eugster, W., and Chapin, F. S.: A regional study of the controls on water vapor and CO_2 exchange in arctic tundra, Ecology, 84, 2762-2776, 2003.

McGuire, A. D., Wirth, C., Apps, M., Beringer, J., Clein, J., Epstein, H., Kicklighter, D. W., Bhatti, J., Chapin, F. S., de
30 Groot, B., Efremov, D., Eugster, W., Fukuda, M., Gower, T., Hinzman, L., Huntley, B., Jia, G. J., Kasischke, E., Melillo, J., Romanovsky, V., Shvidenko, A., Vaganov, E., and Walker, D.: Environmental variation, vegetation distribution, carbon dynamics and water/energy exchange at high latitudes, J. Veg. Sci., 13, 301-314, 2002.

Merbold, L., Kutsch, W. L., Corradi, C., Kolle, O., Rebmann, C., Stoy, P. C., Zimov, S. A., and Schulze, E. D.: Artificial drainage and associated carbon fluxes (CO_2/CH_4) in a tundra ecosystem, Glob. Change Biol., 15, 2599-2614, 2009.

35 Muster, S., Langer, M., Heim, B., Westermann, S., and Boike, J.: Subpixel Heterogeneity of Ice-Wedge Polygonal Tundra: A Multi-Scale Analysis of Land Cover and Evapotranspiration in the Lena River Delta, Siberia, Tellus B, 64, 17301, 2012.

Muster, S., Heim, B., Abnizova, A., and Boike, J.: Water Body Distributions Across Scales: A Remote Sensing Based Comparison of Three Arctic Tundra Wetlands, Rem. Sens., 5, 1498-1523, 2013.

Myers-Smith, I. H., Forbes, B. C., Wilmking, M., Hallinger, M., Lantz, T., Blok, D., Tape, K. D., Macias-Fauria, M., Sass-
40 Klaassen, U., Levesque, E., Boudreau, S., Ropars, P., Hermanutz, L., Trant, A., Collier, L. S., Weijers, S., Rozema, J., Rayback, S. A., Schmidt, N. M., Schaepman-Strub, G., Wipf, S., Rixen, C., Menard, C. B., Venn, S., Goetz, S., Andreu-

Hayles, L., Elmendorf, S., Ravolainen, V., Welker, J., Grogan, P., Epstein, H. E., and Hik, D. S.: Shrub expansion in tundra ecosystems: dynamics, impacts and research priorities, Environ. Res. Lett., 6, 2011.

Myers-Smith, I. H., and Hik, D. S.: Shrub canopies influence soil temperatures but not nutrient dynamics: An experimental test of tundra snow-shrub interactions, Ecol. Evol., 3, 3683-3700, 2013.

5   Natali, S. M., Schuur, E. A. G., Mauritz, M., Schade, J. D., Celis, G., Crummer, K. G., Johnston, C., Krapek, J., Pegoraro, E., Salmon, V. G., and Webb, E. E.: Permafrost thaw and soil moisture driving CO2 and CH4 release from upland tundra, J. Geophys. Res.-Biogeo., 120, 525-537, 2015.

O'Donnell, J. A., Jorgenson, M. T., Harden, J. W., McGuire, A. D., Kanevskiy, M. Z., and Wickland, K. P.: The Effects of Permafrost Thaw on Soil Hydrologic, Thermal, and Carbon Dynamics in an Alaskan Peatland, Ecosystems, 15, 213-229, 10   2012.

Oberbauer, S. F., Tweedie, C. E., Welker, J. M., Fahnestock, J. T., Henry, G. H. R., Webber, P. J., Hollister, R. D., Walker, M. D., Kuchy, A., Elmore, E., and Starr, G.: Tundra CO2 fluxes in response to experimental warming across latitudinal and moisture gradients, Ecol. Monogr., 77, 221-238, 2007.

Oechel, W. C., Vourlitis, G. L., Hastings, S. J., Ault, R. P., and Bryant, P.: The effects of water table manipulation and 15   elevated temperature on the net CO2 flux of wet sedge tundra ecosystems, Glob. Change Biol., 4, 77-90, 1998.

Olivas, P. C., Oberbauer, S. F., Tweedie, C. E., Oechel, W. C., and Kuchy, A.: Responses of CO2 flux components of Alaskan Coastal Plain tundra to shifts in water table, J. Geophys. Res.-Biogeo., 115, 2010.

Ping, C.-L., Michaelson, G. J., Jorgenson, M. T., Kimble, J. M., Epstein, H., Romanovsky, V. E., and Walker, D. A.: High stocks of soil organic carbon in the North American Arctic region, Nat. Geosci., 1, 615-619, 2008.

20   Pithan, F., and Mauritsen, T.: Arctic amplification dominated by temperature feedbacks in contemporary climate models, Nat. Geosci., 7, 181-184, 2014.

Polyakov, I. V., Bekryaev, R. V., Alekseev, G. V., Bhatt, U. S., Colony, R. L., Johnson, M. A., Maskshtas, A. P., and Walsh, D.: Variability and trends of air temperature and pressure in the maritime Arctic, 1875-2000, J. Clim., 16, 2067-2077, 2003.

Pomeroy, J. W., Bewley, D. S., Essery, R. L. H., Hedstrom, N. R., Link, T., Granger, R. J., Sicart, J. E., Ellis, C. R., and 25   Janowicz, J. R.: Shrub tundra snowmelt, Hydrol. Proc., 20, 923-941, 2006.

Rasilo, T., Prairie, Y. T., and del Giorgio, P. A.: Large-scale patterns in summer diffusive CH4 fluxes across boreal lakes, and contribution to diffusive C emissions, Glob. Change Biol., 21, 1124-1139, 2015.

Rawlins, M. A., McGuire, A. D., Kimball, J. S., Dass, P., Lawrence, D., Burke, E., Chen, X., Delire, C., Koven, C., MacDougall, A., Peng, S., Rinke, A., Saito, K., Zhang, W., Alkama, R., Bohn, T. J., Ciais, P., Decharme, B., Gouttevin, I., 30   Hajima, T., Ji, D., Krinner, G., Lettenmaier, D. P., Miller, P., Moore, J. C., Smith, B., and Sueyoshi, T.: Assessment of model estimates of land-atmosphere CO2 exchange across Northern Eurasia, Biogeosciences, 12, 4385-4405, 2015.

Rouse, W. R., Carlson, D. W., and Weick, E. J.: Impacts of summer warming on the energy and water-balance of wetland tundra, Clim. Change, 22, 305-326, 1992.

Rouse, W. R.: The energy and water balance of high-latitude wetlands: controls and extrapolation, Glob. Change Biol., 6, 35   59-68, 2000.

Schuur, E. A. G., Bockheim, J., Canadell, J. G., Euskirchen, E., Field, C. B., Goryachkin, S. V., Hagemann, S., Kuhry, P., Lafleur, P. M., Lee, H., Mazhitova, G., Nelson, F. E., Rinke, A., Romanovsky, V. E., Shiklomanov, N., Tarnocai, C., Venevsky, S., Vogel, J. G., and Zimov, S. A.: Vulnerability of permafrost carbon to climate change: Implications for the global carbon cycle, Bioscience, 58, 701-714, 2008.

40   Schuur, E. A. G., and Abbott, B.: High risk of permafrost thaw, Nature, 480, 32-33, 2011.

Schuur, E. A. G., McGuire, A. D., Schaedel, C., Grosse, G., Harden, J. W., Hayes, D. J., Hugelius, G., Koven, C. D., Kuhry, P., Lawrence, D. M., Natali, S. M., Olefeldt, D., Romanovsky, V. E., Schaefer, K., Turetsky, M. R., Treat, C. C., and Vonk, J. E.: Climate change and the permafrost carbon feedback, Nature, 520, 171-179, 2015.

Semiletov, I. P., Shakhova, N. E., Sergienko, V. I., Pipko, II, and Dudarev, O. V.: On carbon transport and fate in the East
5 Siberian Arctic land-shelf-atmosphere system, Environ. Res. Lett., 7, 2012.

Serreze, M. C., Walsh, J. E., Chapin, F. S., Osterkamp, T., Dyurgerov, M., Romanovsky, V., Oechel, W. C., Morison, J., Zhang, T., and Barry, R. G.: Observational evidence of recent change in the northern high-latitude environment, Clim. Change, 46, 159-207, 2000.

Shaver, G. R., Billings, W. D., Chapin, F. S., Giblin, A. E., Nadelhoffer, K. J., Oechel, W. C., and Rastetter, E. B.: Global
10 change and the carbon balance of Arctic ecosystems, Bioscience, 42, 433-441, 1992.

Shiklomanov, N. I., Streletskiy, D. A., Nelson, F. E., Hollister, R. D., Romanovsky, V. E., Tweedie, C. E., Bockheim, J. G., and Brown, J.: Decadal variations of active-layer thickness in moisture-controlled landscapes, Barrow, Alaska, J. Geophys. Res.-Biogeo., 115, 2010.

Strauss, J., Schirrmeister, L., Grosse, G., Wetterich, S., Ulrich, M., Herzschuh, U., and Hubberten, H.-W.: The deep
15 permafrost carbon pool of the Yedoma region in Siberia and Alaska, Geophys. Res. Lett., 40, 6165-6170, 2013.

Stull, R. B.: An Introduction to Boundary Layer Meteorology, Atmospheric Sciences Library, Kluwer Academic Publishers, Dordrecht, Boston, London, 670 pp., 1988.

Sturm, M., McFadden, J. P., Liston, G. E., Chapin, F. S., Racine, C. H., and Holmgren, J.: Snow-shrub interactions in Arctic tundra: A hypothesis with climatic implications, J. Clim., 14, 336-344, 2001a.

20 Sturm, M., Racine, C., and Tape, K.: Climate change - Increasing shrub abundance in the Arctic, Nature, 411, 546-547, 2001b.

Sturm, M., Douglas, T., Racine, C., and Liston, G. E.: Changing snow and shrub conditions affect albedo with global implications, J. Geophys. Res.-Biogeo., 110, 2005a.

Sturm, M., Schimel, J., Michaelson, G., Welker, J. M., Oberbauer, S. F., Liston, G. E., Fahnestock, J., and Romanovsky, V.
25 E.: Winter biological processes could help convert arctic tundra to shrubland, Bioscience, 55, 17-26, 2005b.

Sturtevant, C. S., Oechel, W. C., Zona, D., Kim, Y., and Emerson, C. E.: Soil moisture control over autumn season methane flux, Arctic Coastal Plain of Alaska, Biogeosciences, 9, 1423-1440, 2012.

Subin, Z. M., Koven, C. D., Riley, W. J., Torn, M. S., Lawrence, D. M., and Swenson, S. C.: Effects of Soil Moisture on the Responses of Soil Temperatures to Climate Change in Cold Regions, J. Clim., 26, 3139-3158, 2013.

30 Trenberth, K. E., and Fasullo, J. T.: An apparent hiatus in global warming?, Earth Future, 1, 19-32, 2013.

Trenberth, K. E., Fasullo, J. T., Branstator, G., and Phillips, A. S.: Seasonal aspects of the recent pause in surface warming, Nat. Clim. Change, 4, 911-916, 2014.

Turetsky, M. R., Treat, C. C., Waldrop, M. P., Waddington, J. M., Harden, J. W., and McGuire, A. D.: Short-term response of methane fluxes and methanogen activity to water table and soil warming manipulations in an Alaskan peatland, J.
35 Geophys. Res.-Biogeo., 113, n/a-n/a, 2008.

van Huissteden, J., and Dolman, A. J.: Soil carbon in the Arctic and the permafrost carbon feedback, Curr. Opin. Environ. Sustain., 4, 545-551, 2012.

Walter-Anthony, K. M., Zimov, S. A., Grosse, G., Jones, M. C., Anthony, P. M., Iii, F. S. C., Finlay, J. C., Mack, M. C., Davydov, S., Frenzel, P., and Frolking, S.: A shift of thermokarst lakes from carbon sources to sinks during the Holocene
40 epoch, Nature, 511, 452-456, 2014.

Zimov, S. A., Voropaev, Y. V., Semiletov, I. P., Davidov, S. P., Prosiannikov, S. F., Chapin, F. S., Chapin, M. C., Trumbore, S., and Tyler, S.: North Siberian lakes: A methane source fueled by Pleistocene carbon, Science, 277, 800-802, 1997.

Zona, D., Lipson, D. A., Zulueta, R. C., Oberbauer, S. F., and Oechel, W. C.: Microtopographic controls on ecosystem functioning in the Arctic Coastal Plain, J. Geophys. Res.-Biogeo., 116, 2011a.

Zona, D., Oechel, W. C., Richards, J. H., Hastings, S., Kopetz, I., Ikawa, H., and Oberbauer, S.: Light-stress avoidance mechanisms in a Sphagnum-dominated wet coastal Arctic tundra ecosystem in Alaska, Ecology, 92, 633-644, 2011b.

Table 1: Relative abundance of the major vascular plant species found within both disturbance regimes in the context of a non-destructive sampling campaign in 2014. The statistics exclude mosses, dead plants and bare soil, as well as other plant species with a coverage fraction much smaller than one percent.

Species name	Common name	drained area [%]	control area [%]
Betula nana subsp. exilis	Arctic dwarf birch	9.3 ±21.1	0.6 ±2.8
Calamagrostis canadensis	Canadian reedgrass	4.3 ±19.3	0.3 ±1.4
Carex appendiculata and *lugens*	(Tussock forming sedge)	49.2 ±42.8	35.7 ±46.5
Chamaedaphne calyculata	Leatherleaf	3.4 ±10.7	0.4 ±1.3
Eriophorum angustifolium	Common cottongrass	18.6 ±29.0	43.3 ±37.7
Potentila palustris	Marsh cinquefoil	2.3 ±8.1	9.3 ±20.7
Salix myrtilifolia	Common osier	11.4 ±14.5	10.3 ±14.6
Salix pulchra	Diamondleaf willow	1.6 ±6.3	0.0 ±0.0

Table 2: Definition of sub-seasons that reflect the pattern in albedo differences between drainage and control areas. Differences for albedo and net shortwave radiation budget SW(net) were calculated as seasonal means of daily values, drainage minus control. Dates reflect the conditions in data year 2014, and may changes between years.

period	start date	end date	duration [days]	albedo difference [-]	SW(net) difference [Wm^{-2}]
closed snow cover	2/14	4/27	73	2.4	-2.30
thinning of snow cover	4/28	5/22	25	-2.6	7.47
snow cover disappears	5/23	5/31	9	-15.3	48.31
flooding transition	6/1	6/18	18	0.2	-0.54
snow free season	6/19	9/28	102	1.9	-2.18
first snow patches	9/29	10/12	14	3.4	-0.98
snow cover buildup	10/13	10/30	18	12.1	-2.41

Table 3: Energy flux components averaged over the summer months (June-September) within data years 2014 and 2015, including average and relative differences between drainage and control area observations.

parameter	drainage	control	difference	change [%]
Net radiation, R_{net} [Wm^{-2}]	94.0	95.7	-1.7	-1.8
Sensible heat flux, H [Wm^{-2}]	28.4	24.4	4.0	16.7
Latent heat flux, LE [Wm^{-2}]	27.8	27.3	0.5	1.8
Sum of H + LE [Wm^{-2}]	56.2	51.7	4.5	8.8
Bowen Ratio, BR [-]	1.022	0.892	0.131	14.7
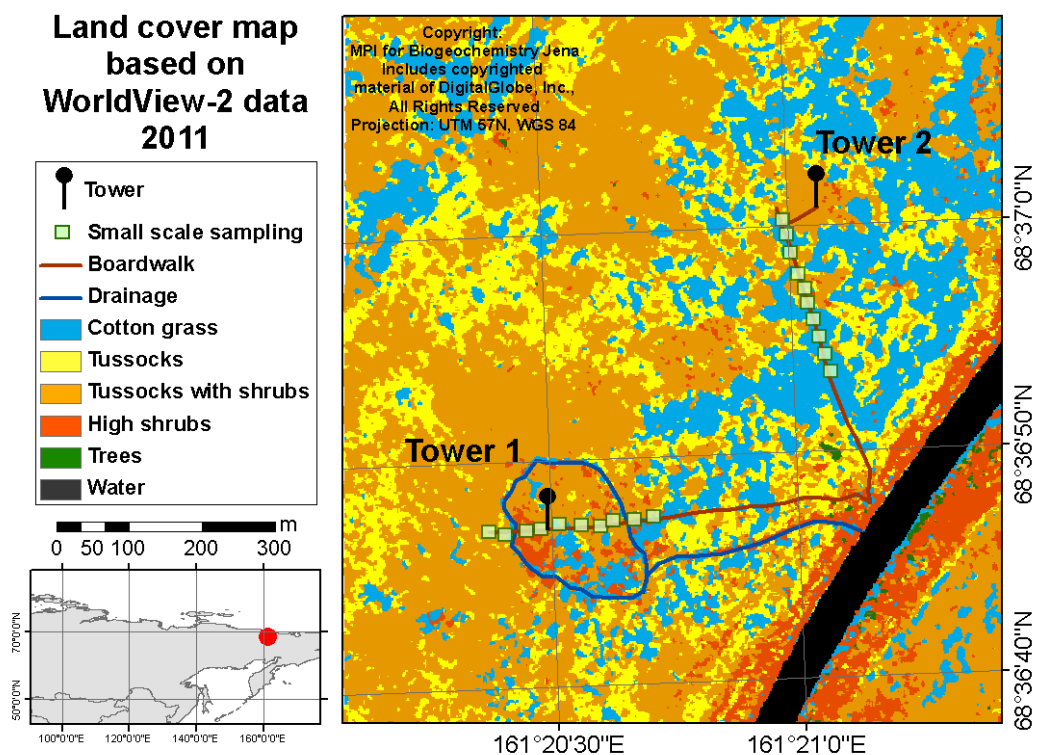
Figure 1: Land cover structure and instrumentation setup at the Chersky observation site.
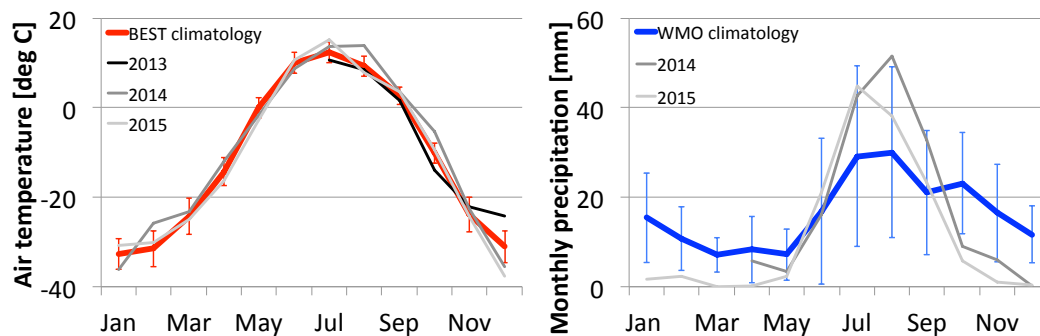
Figure 2: Left panel: Average annual course and recent observations of monthly mean surface temperature (Tair, 1960-2009); right panel: Long-term average and recent observations of monthly precipitation sums (PRCP, 1950-1999) for the Chersky region.
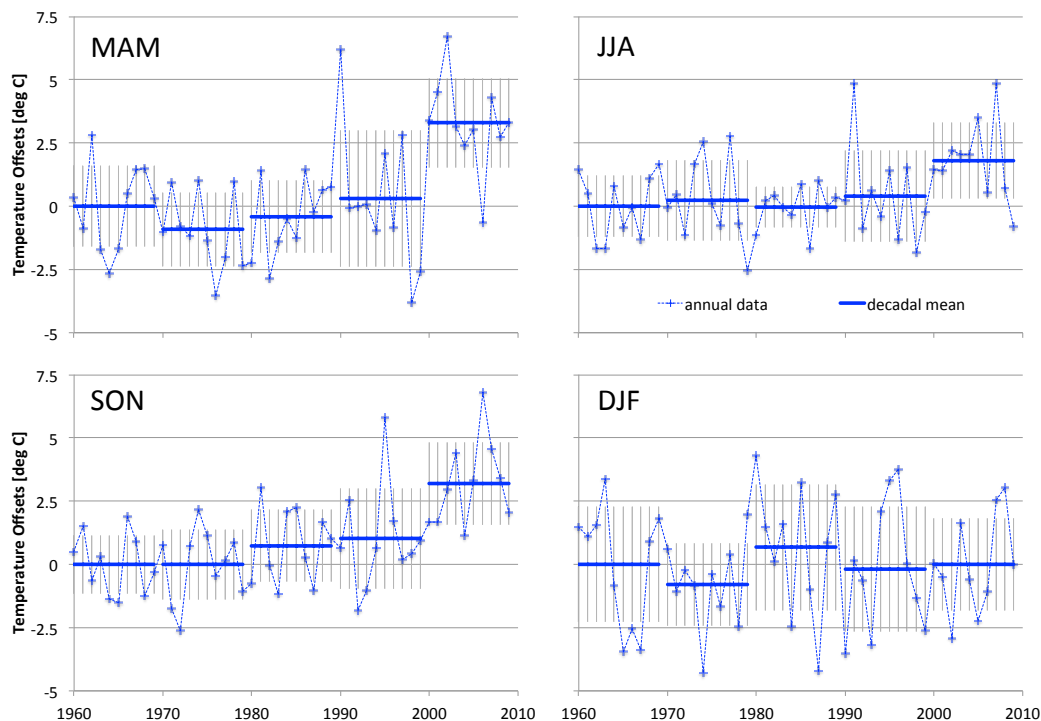
Figure 3: Temperature trends for the Chersky station, taken from the BEST database. Top left: springtime warming period; top right: core summer period; bottom left: fall freeze-up period; bottom right: core winter period. All temperatures were normalized against the mean seasonal temperatures from the 1960-69 decade. Blue crosses and dashed blue lines give annual data, thick blue lines the decadal mean with vertical grey bars showing decadal RMSE.
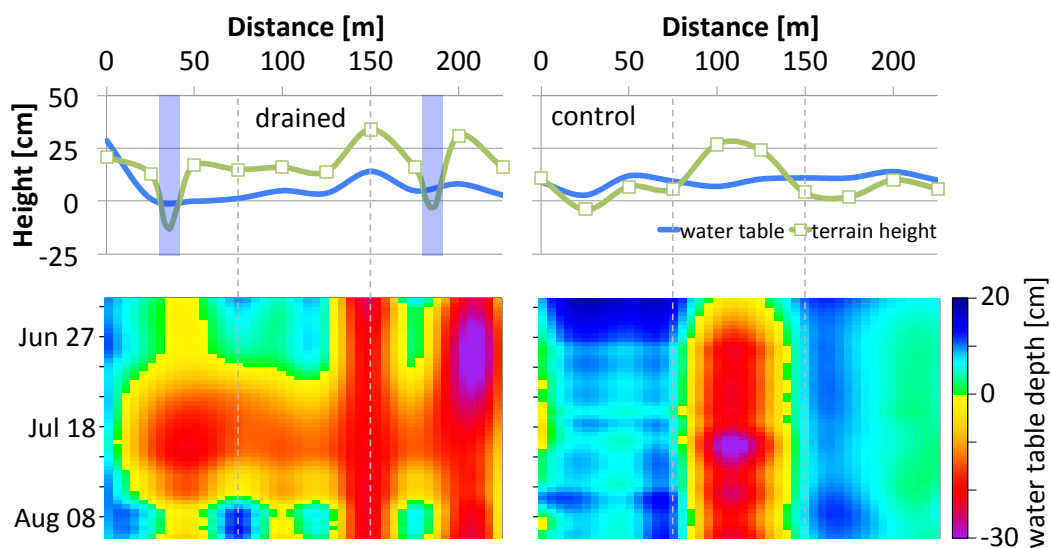
Figure 4: Top panels: Variability of terrain height (green lines, boxes indicating microsite study positions) and water table depth (blue lines) along transects in the drained (left) and control (right) sections of the observation site (water table depth reflects conditions in mid July 2014). Blue shading in drained panel indicates position of drainage channel, where interpolation of terrain height was modified; bottom panels: Development of water table depth over time for the period Jun 18 to Aug 14, 2014 (interpolated over both space and time). Values are given relative to the surface, with negative values indicating water table below the surface level.
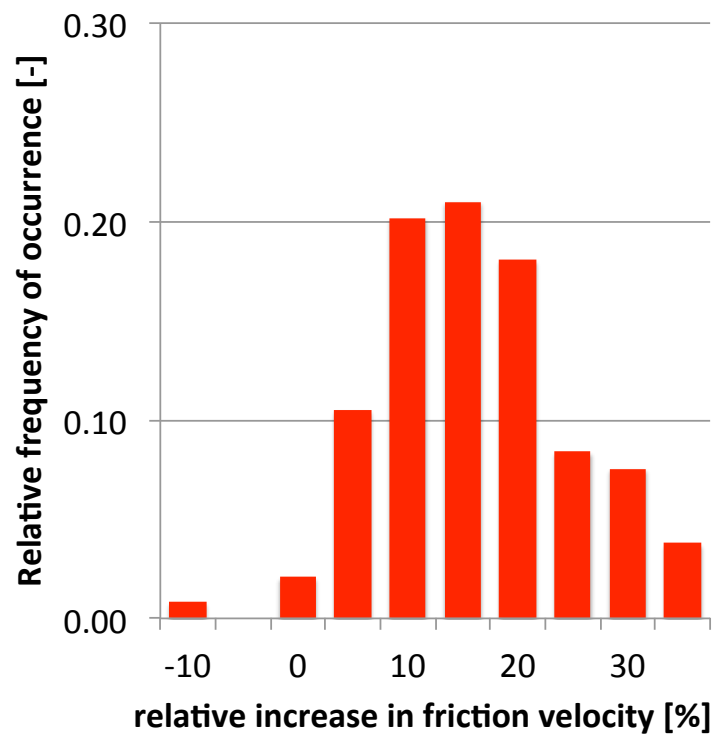
Figure 5: Frequency distribution of the relative increase (drained-control)/control [%]) in friction velocity in the drained area, compared to the control area. Data covers the months June through September in 2014/15.
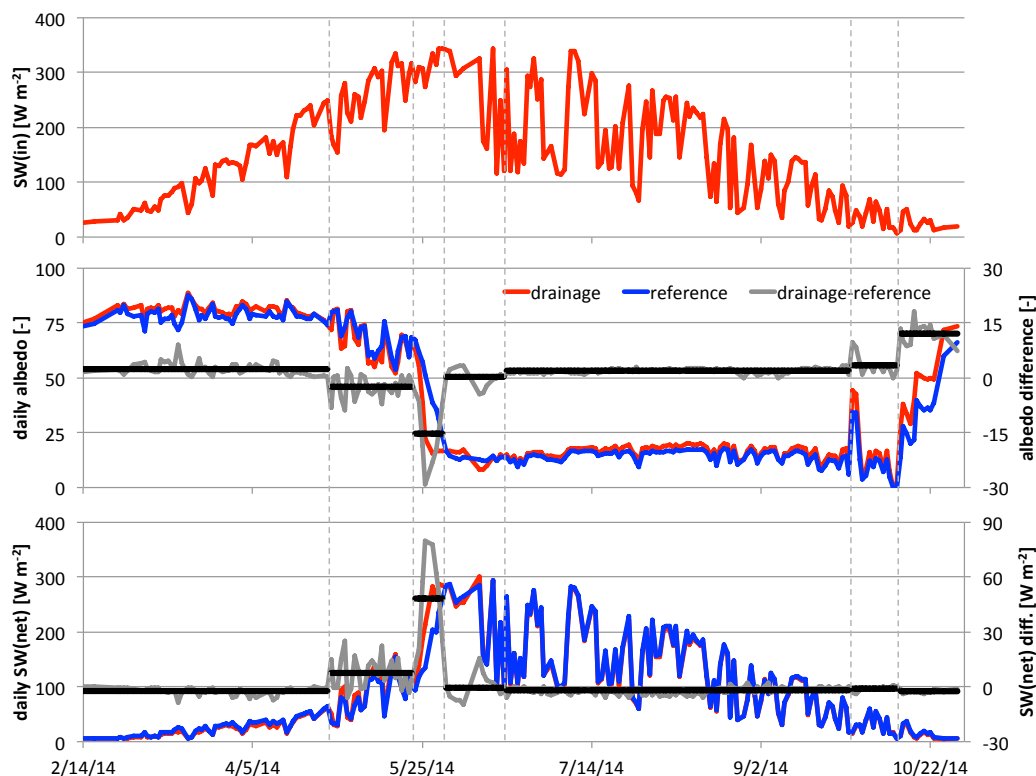
Figure 6: (top) 2014 annual course of the daily mean incoming shortwave radiation; (center) daily mean albedo derived from the ratio of downward and upward shortwave radiation. The grey line indicates the daily difference between drained and control towers (scales on the right), with the black horizontal bars giving the mean values for seven sub-seasons (separated by vertical dashed lines, see Table 2 for definitions); (bottom) same structure as used in the center panel, here to show the net shortwave radiation budget from both towers and their seasonal differences. All plots have been restricted to the period where SW(in) > 5 Wm^{-2}.
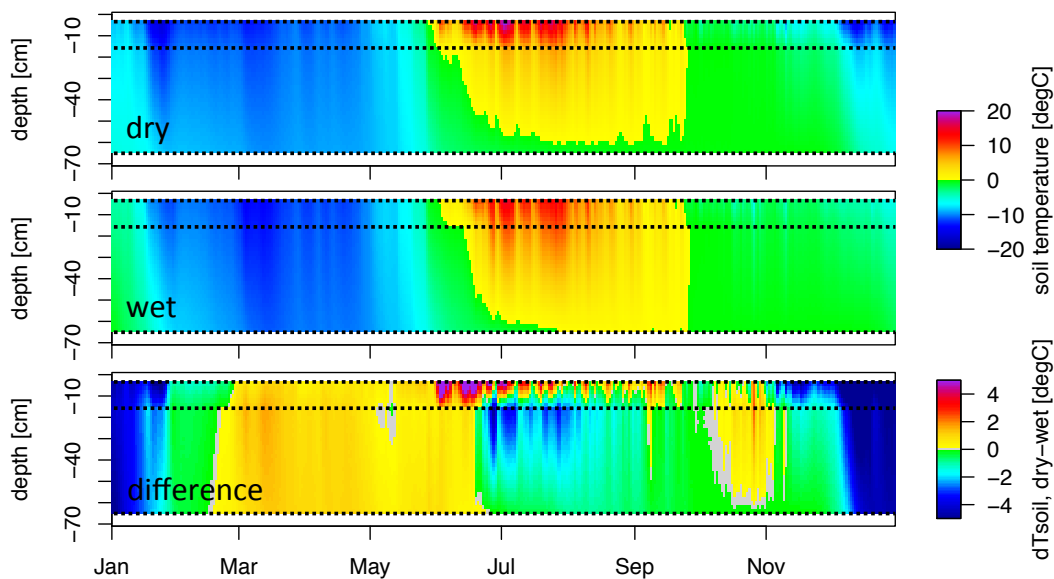
Figure 7: **Daily mean soil temperature profiles at a dry (upper panel) and wet (center panel) microsite within the drained transect, and the difference (dry-wet, bottom panel) for the calendar year 2015. Data for three measurement depths (dotted lines) are linearly interpolated along the vertical profile. Values in the difference plot were truncated to the range [-5; 5] degC to enhance visibility of fine-scale patterns, while values fell within the range [-11.3; 10.5] degC.**
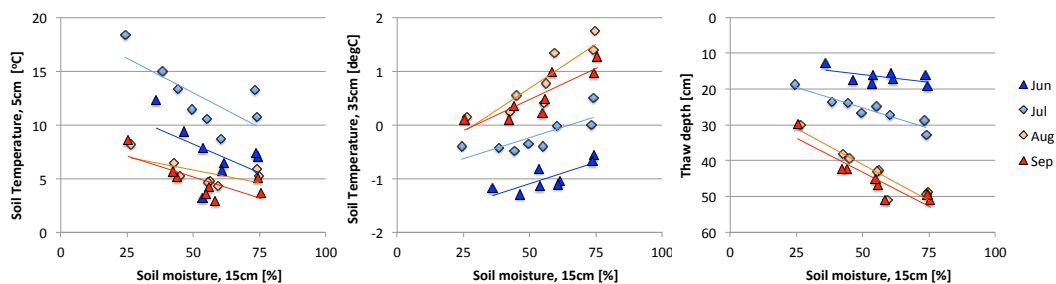
Figure 8: Influence of soil moisture on soil temperatures and thaw depth at eight microsites covering both disturbance treatments. Observations from summer 2015 are aggregated by site over a period of about two weeks each (Jun 13-30; Jul 01-13; Aug 21-31; Sep 01-12). Lines represent linear regression fits to emphasize trends.
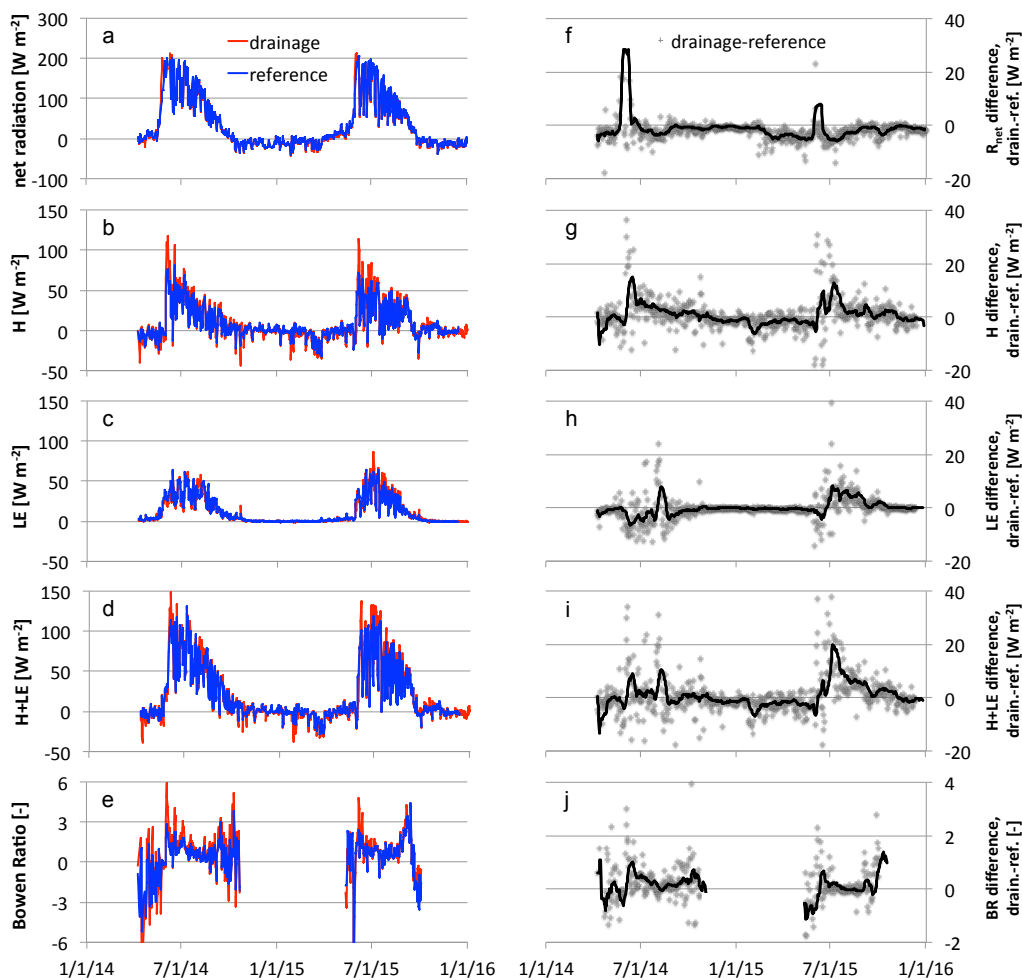
Figure 9: (a-e) Summary of daily averaged energy fluxes within drainage (red line) and control (blue line) areas. **(f-j)** Daily differences (drainage minus control, grey crosses) between the two treatments, with black lines giving the average differences for a 15-day moving window. (a, f) net radiation; (b, g) sensible heat fluxes; (c, h) latent heat fluxes; (d, i) sum of sensible and latent heat fluxes; (e, j) Bowen ratio, i.e. ratio of sensible to latent heat fluxes. Vertical scales of difference plots have been truncated to enhance display of fine-scale patterns in overall trends.
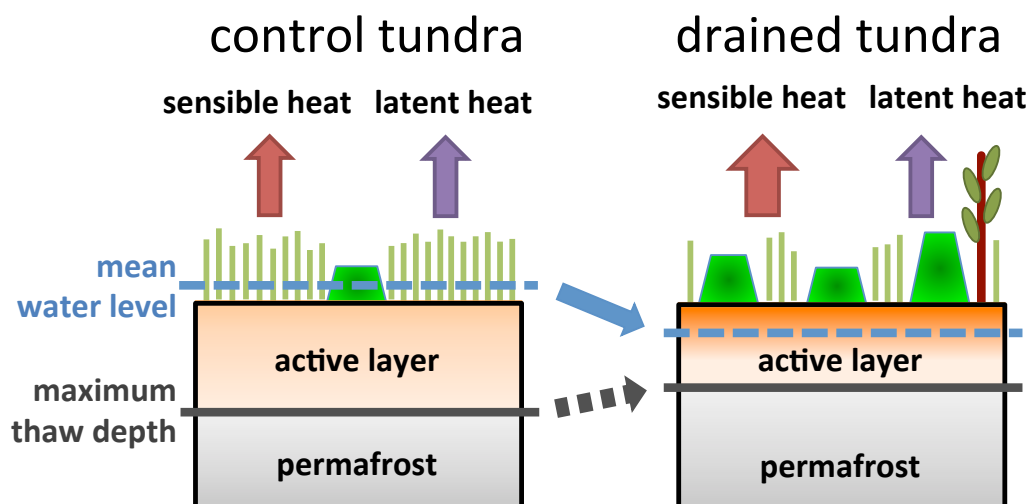
Figure 10: Expected changes in growing season properties of a tundra ecosystem as response to drainage disturbance.